Nucleic Acids Research, 2023, **51**, 10846–10866
https://doi.org/10.1093/nar/gkad837
Advance access publication date: 18 October 2023
Chemical Biology and Nucleic Acid Chemistry

Unprecedented reactivity of polyamines with aldehydic DNA modifications: structural determinants of reactivity, characterization and enzymatic stability of adducts

Eka Putra Gusti Ngurah Putu [1,2], Laurent Cattiaux [1,2], Thomas Lavergne [3], Yves Pommier [4], Sophie Bombard [1,2] and Anton Granzhan [1,2,*]

[1]CMBC, CNRS UMR9187, INSERM U1196, Institut Curie, PSL Research University, 91405 Orsay, France
[2]CMBC, CNRS UMR9187, INSERM U1196, Université Paris Saclay, 91405 Orsay, France
[3]DCM, CNRS UMR5250, Université Grenoble Alpes, 38000 Grenoble, France
[4]Laboratory of Molecular Pharmacology & Developmental Therapeutics Branch, CCR-NCI, NIH, Bethesda, MD 20892, USA

[*]To whom correspondence should be addressed. Tel: +33 1 69 86 30 89; Email: anton.granzhan@curie.fr
Disclaimer: This publication reflects only the authors' view and the European Research Agency is not responsible for any use that may be made of the information it contains.

Abstract

Apurinic/apyrimidinic (AP) sites, 5-formyluracil (fU) and 5-formylcytosine (fC) are abundant DNA modifications that share aldehyde-type reactivity. Here, we demonstrate that polyamines featuring at least one secondary 1,2-diamine fragment in combination with aromatic units form covalent DNA adducts upon reaction with AP sites (with concomitant cleavage of the AP strand), fU and, to a lesser extent, fC residues. Using small-molecule mimics of AP site and fU, we show that reaction of secondary 1,2-diamines with AP sites leads to the formation of unprecedented 3′-tetrahydrofuro[2,3,4-*ef*]-1,4-diazepane ('ribodiazepane') scaffold, whereas the reaction with fU produces cationic 2,3-dihydro-1,4-diazepinium adducts via uracil ring opening. The reactivity of polyamines towards AP sites versus fU and fC can be tuned by modulating their chemical structure and pH of the reaction medium, enabling up to 20-fold chemoselectivity for AP sites with respect to fU and fC. This reaction is efficient in near-physiological conditions at low-micromolar concentration of polyamines and tolerant to the presence of a large excess of unmodified DNA. Remarkably, 3′-ribodiazepane adducts are chemically stable and resistant to the action of apurinic/apyrimidinic endonuclease 1 (APE1) and tyrosyl-DNA phosphoesterase 1 (TDP1), two DNA repair enzymes known to cleanse a variety of 3′ end-blocking DNA lesions.

Graphical abstract

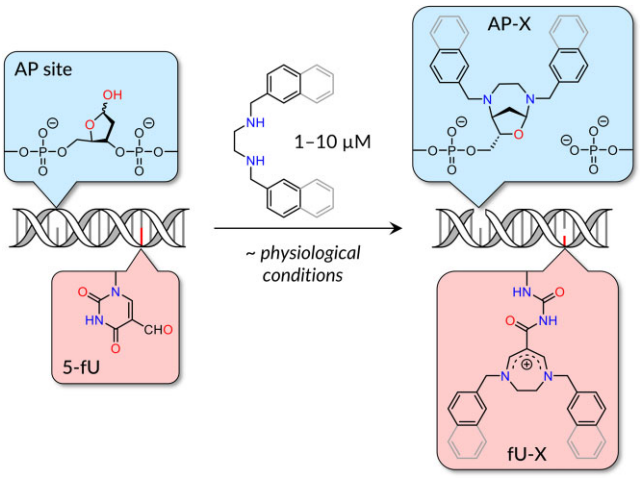

Introduction

Abasic (apurinic/apyrimidinic, hereafter AP) sites represent one of the most abundant DNA lesions that are formed upon spontaneous depurination of DNA (1), enzymatic removal of damaged (deaminated, oxidized, or alkylated) nucleobases (2–5), and active demethylation of epigenetic marks (6,7). The rate of AP sites formation is estimated as about 10 000–20 000 per cell per day (3,4). AP sites are non-coding and, if left unrepaired, represent roadblocks to RNA polymerases and induce mutations upon DNA replication. AP sites exist

Received: May 23, 2023. **Revised:** September 14, 2023. **Editorial Decision:** September 15, 2023. **Accepted:** September 20, 2023

in an equilibrium between the ring-closed hemiacetal and the ring-open aldehyde forms (Figure 1A) (8). Although the aldehyde form represents only about 1% at physiological conditions, its high reactivity leads to multiple reaction pathways resulting in formation of various products, including *inter alia* interstrand DNA crosslinks (ICLs) via reactions with adjacent nucleobases (9–14), DNA–protein crosslinks (DPCs) via reactions with lysine and cysteine residues of proteins (15–21), in particular histones (22–24), as well as DNA strand breaks via β-elimination of the 3′-phosphate group and formation of the *trans*-α,β-unsaturated aldehyde remnant on the 3′ DNA terminus (3′-PUA, Figure 1A) (25). Notably, 3′-PUA is even more reactive than the uncleaved AP site, giving rise to the formation of chemically distinct DNA ICLs (26,27), DPCs (28–33), as well as 3′-glutathionylation of DNA in cellular conditions (34).

Considering the importance of AP sites as key intermediates in DNA repair, several methods have been developed to chemically label these residues, in order to quantify their abundance in genomic DNA by bulk methods such as fluorimetry (35–39), chemiluminescence (40), ELISA-like assays (41–45) or mass spectrometry (46,47), or to visualize them in cells by fluorescence microscopy (48). Recently, two distinct strategies, AP-seq (49) and snAP-seq (50), both based on chemical labelling of AP sites were employed to isolate the AP site-containing DNA fragments by affinity precipitation and to map them to the genome via DNA sequencing, allowing to study the genomic distribution of AP sites. Notably, in most cases, chemical labelling of AP sites relies on the formation of oxime-type adducts through the reaction with oxyamine derivatives endowed with a fluorophore, a bioorthogonal ('clickable') handle, or an affinity tag (biotin). However, this reaction has limited chemoselectivity, as oxyamines may also react with two other aldehyde-containing DNA modifications, namely 5-formyluracil (fU) and 5-formylcytosine (fC, Figure 1B) (51). Selective labelling of AP sites therefore requires a rigorous maintenance of strict reaction conditions or, in the case of snAP-seq, a sophisticated multi-step protocol to remove the products of reaction of the probe with fU residues (50). Recently, Li *et al.* proposed a novel strategy for chemical labelling of aldehyde residues in DNA based on the formation of fluorescent 1,2-dihydroquinazoline-3-oxides upon reaction with 2-aminobenzamidoxime (ABAO) probe ('ABAO ligation'); however, this reaction also occurs with fU and fC residues, showing poor selectivity for AP sites (52). On the other hand, chemoselective labelling of fU and fC has been successfully achieved, enabling the determination of their abundance and genomic distribution (53–56). Thus, there is a need to develop efficient, operationally simple and highly selective strategies for chemical labelling of AP sites.

Along these lines, we recently investigated the interaction of AP site-containing DNA duplexes with a series of polyazanaphthalenophanes. These compounds bind non-covalently to AP sites with high affinity and selectivity, interfere with their enzymatic repair, and promote the cleavage of AP sites by β- and/or β,δ-elimination mechanisms with various efficiency, depending on their precise chemical structure (57–59). In the course of our investigations, we fortuitously observed that one of naphthalenophanes, BisNP-NH, not only promoted the cleavage of AP sites, but led to the formation of an unexpected covalent adduct with the cleaved AP site in the absence of reducing agents (AP-X, Figure 1C), with a yield of up to 60% (59). Intrigued by this unusual reactivity, we sought a more detailed investigation of this phenomenon and its suitability for selective labelling of AP sites. In the present study, we identified structural determinants for the reaction of polyamines with AP sites, fU and fC, elucidated chemical structures of the corresponding adducts, investigated the influence of reaction conditions on the formation of adducts, and assessed their chemical and enzymatic stability. We show that polyamines containing a secondary 1,2-diamine fragment in combination with aromatic moieties can efficiently react with AP sites and fU residues leading to chemically distinct and, in the case of reaction with AP sites, chemically and enzymatically stable adducts. Importantly, the AP-vs.-fU selectivity of polyamines can be finely tuned by modifying chemical structure of the polyamine reagents and reaction conditions, allowing preferential reactivity with AP sites with a satisfactory chemoselectivity.

Materials and methods

Chemicals

Synthesis of BisNP-NH × 6 HCl and BisNP-O × 4 HCl has been described previously (60). Synthesis of BisNP-NH/O × 5 HCl is described in Supplementary Information. BisNP-$\frac{1}{2}$ × 3 HCl, C2N2 × 2 HCl, C33N3 × 3 HCl and DBDT × 3 HCl were prepared following the literature procedures (61,62); the identity and purity of all compounds synthesized in-house was confirmed by ^{1}H NMR, LC/MS, and combustion microanalysis. 1,7-Dibenzylethylenediamine (DBED) × 2 AcOH, 1,4,7-triazacyclononane (TACN) × 3 HCl, cyclen × 4 HCl and hexacyclen × 6 HCl were purchased from TCI and used without additional purification. Stock solutions of polyamine salts were prepared in deionized water at a concentration of 2–5 mM and stored at 4°C.

Preparative-scale synthesis of 3α and 3β

To a solution of (*S*,*E*)-5-*O*-TBDPS-4,5-dihydroxypent-2-enal **2** (52 mg, 0.15 mmol, 1 equiv.) (63) in a mixture of MeCN and H_2O (9:1 v/v, 5.9 ml) was added DBED diacetate (53 mg, 0.15 mmol, 1 equiv.) and K_2CO_3 (43 mg, 0.31 mmol, 2.1 equiv.). The reaction mixture was stirred at 40°C for 3 days and then concentrated to dryness. The residue was dissolved in a mixture of DCM/H_2O (1:1, 6 ml). The organic layer was separated and the aqueous layer was extracted with DCM (3 × 3 ml). The organic layers were combined, dried over $MgSO_4$, filtered and concentrated. The residue was purified by column chromatography on silica gel (eluent: cyclohexane–AcOEt, 100:0 to 90:10) giving first a fraction containing **3β** (12 mg), following by a mixture of **3α** and **3β** (41 mg) and a fraction containing the pure **3α** (17 mg), with an overall yield of 83% for both diastereomers.

Ribodiazepane **3α**: Pale yellow oil, R_f = 0.50 (cyclohexane–AcOEt 80:20); ^{1}H NMR (300 MHz, $CDCl_3$): δ 7.64–7.58 (m, 4H, H_{Ar}), 7.44–7.22 (m, 16H, H_{Ar}), 5.02 (d, J = 7.1 Hz, 1H, H^1), 4.24 (dd, J = 6.5, 4.1 Hz, 1H, H^4), 3.93 (d, J = 13.9 Hz, 1H, CH_aH_bBn), 3.74 (d, J = 13.9 Hz, 1H, CH_aH_bBn), 3.73 (d, J = 13.9 Hz, 1H, CH_aH_bBn), 3.63 (d, 1H, J = 14.1 Hz, CH_aH_bBn), 3.58 (dd, J = 10.7, 4.3 Hz, 1H, H^{5a}), 3.51 (d, J = 7.0 Hz, 1H, H_3), 3.42 (dd, J = 10.4, 6.4 Hz, 1H, H^{5b}), 2.92–2.78 (m, 2H, NCH_2CH_2N), 2.69–2.52 (m, 2H, NCH_2CH_2N), 2.15 (d, J = 13.6 Hz, 1H, $H^{2\alpha}$), 1.98 (dd, J = 13.9, 7.2 Hz, $H^{2\beta}$), 1.01 (s, 9H, *t*Bu); ^{13}C NMR (75 MHz, $CDCl_3$): δ 139.6 (C_q), 139.5 (C_q), 135.7 (2 CH), 133.6

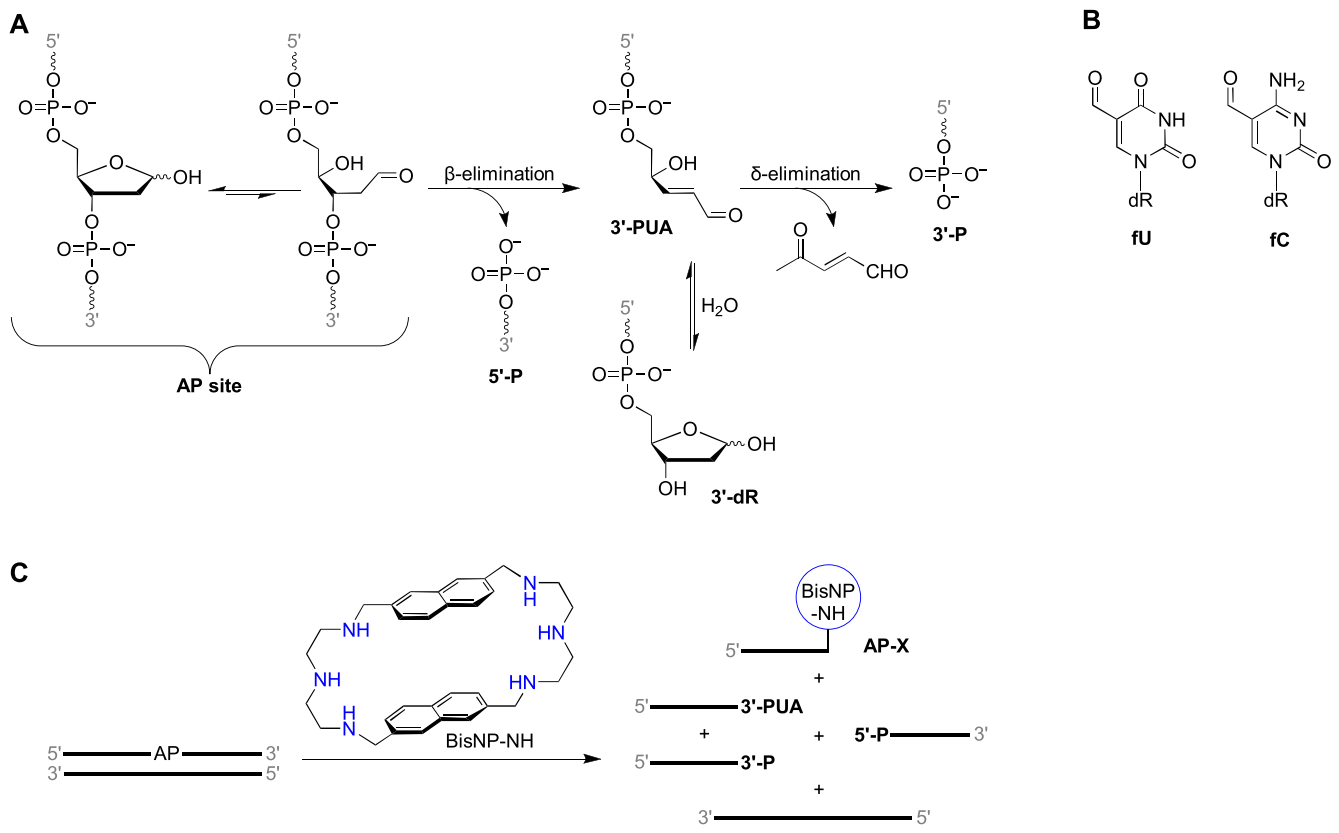

Figure 1. (**A**–**B**) Chemical structures of aldehyde-containing DNA modifications: (**A**) AP site and the products of its degradation including 3′-blocking ends (3′-PUA, 3′-dR, and 3′-P); (**B**) 5-formyluracil (fU) and 5-formylcytosine (fC) residues, dR = deoxyribose fragment. (**C**) Reaction of AP duplex with polyazamacrocycle BisNP-NH leading to cleavage of the AP strand and formation of the BisNP-NH adduct ('AP-X') (59).

(C_q), 133.5 (C_q), 129.8 (CH), 129.8 (CH), 128.9 (CH), 128.9 (CH), 128.4 (CH), 128.4 (CH), 127.8 (CH), 127.8(CH), 127.1 (CH), 127.0 (CH), 94.9 (CH, C-1), 82.4 (CH, weak, C-4), 65.8 (CH_2, C-5), 63.7 (CH, C-3), 61.1 (CH_2, Bn), 58.1 (CH_2, Bn), 49.8 (NCH_2CH_2N), 48.4 (NCH_2CH_2N), 31.5 (CH_2, C-2), 27.0 (CH_3, *t*Bu), 19.4 (C_q, *t*Bu); ESI-HRMS: *m/z* $[M + H]^+$ calculated for $C_{37}H_{45}N_2O_2Si$: 577.3250, found: 577.3227.

Ribodiazepane **3β** : Pale yellow oil, R_f = 0.58 (cyclohexane–AcOEt, 80:20); ^{1}H NMR (300 MHz, $CDCl_3$): δ 7.83–7.67 (m, 4H, H_{Ar}), 7.50–7.08 (m, 16H, H_{Ar}), 5.01 (d, J = 7.8 Hz, 1H, H^1), 4.11–4.05 (m, 2H, H^5), 3.95–3.87 (m, 1H, H^4), 3.84 (d, J = 13.5 Hz, 1H, CH_aH_bBn), 3.63 (s, 2H, CH_2Bn), 3.57 (d, J = 13.5 Hz, 1H, CH_aH_bBn), 3.38 (dd, 1H, J = 6.0, 4.4 Hz, H^3), 2.64–2.56 (m, 2H, NCH_2CH_2N), 2.55– 2.45 (m, 2H, NCH_2CH_2N), 2.30 (d, J = 13.8 Hz, 1H, $H^{2\beta}$), 1.88 (ddd, J = 13.9, 7.9, 6.1 Hz, 1H, $H^{2\alpha}$), 1.07 (s, 9H, *t*Bu); ^{13}C NMR (75 MHz, $CDCl_3$): δ 139.9 (C_q), 139.5 (C_q), 135.9 (CH), 135.8 (CH), 134.2 (C_q), 134.0 (C_q), 129.7 (CH), 129.6 (CH), 129.0 (CH), 129.0 (CH), 128.3 (CH), 128.3 (CH), 127.9 (CH), 127.8 (CH), 127.0 (CH), 127.0 (CH), 94.6 (CH, C-1), 84.5 (CH, C-4), 63.9 (CH_2, C-5), 63.3 (CH_2, Bn), 62.4 (CH, C-3), 59.5 (CH_2, Bn), 51.3 (CH_2, NCH_2CH_2N), 48.7 (CH_2, NCH_2CH_2N), 31.8 (CH_2, C-2), 27.1 (CH_3, *t*Bu), 19.3 (C_q, *t*Bu); ESI-HRMS: *m/z* $[M + H]^+$ calculated for $C_{37}H_{45}N_2O_2Si$: 577.3250, found: 577.3234.

Reaction of AP site mimic 1 with DBED

A solution of 5-*O*-TBDPS-3-*O*-acetyl-2-deoxyribofuranose **1** (6.2 mg, 15 μmol, 25 mM) (63) and DBED diacetate (5.4 mg, 15 μmol, 25 mM) in a mixture of MeCN and sodium phosphate buffer (50 mM, pH 7.0) (9:1 v/v, 600 μl) was stirred at 40°C for 24 h. HPLC analysis (injection volume: 2 μl, column: Waters Atlantis T3 C_{18}, 3 μm, 3.0 × 100 mm; flow rate: 0.8 ml min^{-1}; eluent A: H_2O + 0.1% v/v formic acid, eluent B: MeCN + 0.1% v/v formic acid; 5 to 100% of B over 10 min, detection wavelength: 270 nm). The ratio of diastereomers (**3α:3β** = 97:3) was determined by comparison with the chromatograms of analytically pure samples obtained above, assuming equal extinction coefficients for both diastereomers.

Reaction of 3′-PUA mimic 2 with DBED

A solution of **2** (4.0 mg, 11.3 μmol, 25 mM) and DBED diacetate (4.0 mg, 11.3 μmol, 25 mM) in a mixture of MeCN and sodium phosphate buffer (50 mM, pH 7.0) (9:1 v/v, 450 μl) was stirred at 40°C for 24 h. The ratio of diastereomers (**3α:3β** = 94:6) was determined by HPLC analysis as described above.

Reaction of 1-Me-fU with DBED

To a mixture of MeCN and sodium phosphate buffer (50 mM, pH 7.0) (1:1 v/v, 3.4 ml) were added 1-Me-fU (13.0 mg, 84.4 μmol, 1 equiv.) (64) and DBED diacetate (30.4 mg, 84.4 μmol, 1 equiv.). The mixture was heated at 40°C for 3 days, then concentrated to dryness. The residue was dissolved in MeCN–H_2O (1:1 v/v, 500 μl) and purified by semi-preparative HPLC with serial injections of 40 μl (column: Waters Atlantis T3 C_{18}, 3 μm, 3.0 × 100 mm; flow rate: 0.8 ml min^{-1};

Table 1. DNA oligonucleotides used in this study

Acronym	Sequence (5′ → 3′)
5-GTA	CCAGTTC-GTA-GTAACCC
3-TUC	GGGTTAC-TUC-GAACTGG
3-(fU)AC	GGGTTAC-(fU)AC-GAACTGG
3-TA(fC)	GGGTTAC-TA(fC)-GAACTGG
3-TAC	GGGTTAC-TAC-GAACTGG
3-T(C_{12})C	GGGTTAC-T(C_{12})C-GAACTGG[a]

[a]C_{12} stands for 1,12-dodecanediol spacer ('Spacer C12').

eluent A: H_2O + 0.1% v/v formic acid, eluent B: MeCN + 0.1% v/v formic acid; detection wavelengths: 235 and 336 nm). Fractions were collected and the formate counter-ion was exchanged by addition of aqueous HBr (0.1 M, 844 μl, 84.4 μmol, 1.0 equiv.). The resulting solution was freeze-dried, affording 1,4-dibenzyl-6-(*N*′-methylallophanyl)-2,3-dihydro-1,4-diazepinium bromide **7** (17.4 mg, 37%) as a white foam; ^{1}H NMR (300 MHz, D_2O, ref. TSP): δ 8.55 (s, 2H, N=C*H*), 7.51–7.40 (m, 6H, H_{Ar}), 7.40–7.31 (m, 4H, H_{Ar}), 4.93 (s, 4H, CH_2Bn), 3.60 (br s, 4H, NCH_2CH_2N), 2.86 (s, 3H, Me); ^{13}C NMR (75 MHz, D_2O, ref. MeOH): δ 168.9 (C_q), 159.3 (CH), 156.6 (C_q), 132.4 (C_q), 129.9 (CH), 129.8 (CH), 129.5 (CH), 98.2 (C_q), 65.4 (CH_2), 53.6 (CH_2), 26.7 (CH_3); ESI-HRMS: *m/z* [*M*]$^+$ calculated for $C_{22}H_{25}N_4O_2$: 377.1972, found: 377.1994; anal. calcd. (%) for $C_{22}H_{25}BrN_4O_2 \times 6\ H_2O$: C 46.73, H 6.60, Br 14.13, N 9.91; found: C 46.22, H 4.79, N, 10.00.

Oligonucleotides

The sequences of oligonucleotides used in this work are given in Table 1. 3-(fU)AC (HPLC-purified) was purchased from ATDBio; all other oligonucleotides (HPLC-purified) were purchased from Eurogentec. Oligonucleotides were dissolved in Milli-Q water at concentrations of 100–300 μM and stored at −20°C. 5′-^{32}P radiolabeling of oligonucleotides was performed using 20 pmol of an oligonucleotide substrate, 30 U of T4 polynucleotide kinase (Biosearch Technologies) and 30 μCi of [γ-^{32}P]-ATP (PerkinElmer) in a reaction volume of 10 μl, for 30 min at 37°C. The labeled oligonucleotides were purified by gel exclusion using in-house packed columns of Sephadex G-25 (GE Healthcare, UK). Duplex substrates were prepared by hybridization of modified oligonucleotides (3-TUC, 3-TA(fC), 3-(fU)AC, 3-T(C_{12})C) or unmodified control 3-TAC (40 μM plus the corresponding radiolabeled tracer) with the unlabeled mutual complementary strand (5-GTA, 44 μM) in 50 mM $KAsO_2Me_2$, 50 mM KCl, pH 7.2 buffer for 5 min at 75°C followed by slow cooling to room temperature, and stored at −20°C.

Preparation of the AP duplex

The uracil-containing precursor (3-TUC/5-GTA, 200 nmol) was incubated with 5 U of *Escherichia coli* uracil-DNA glycosylase (UDG, New England Biolabs) in 10 μl of 1X UDG reaction buffer (20 mM Tris–HCl pH 8.0, 1 mM DTT, 1 mM EDTA) for 45 min at 37°C. After the reaction, the generated AP duplex was diluted 10-fold to a final concentration of 2 μM in 10 mM $KAsO_2Me_2$, 150 mM KCl, pH 7.2 buffer, stored at –20°C and used without further purification. The conversion of the precursor was systematically verified using 0.5 M NaOH treatment, which induces a complete cleavage of the AP strand without affecting the uracil precursor.

Reactions of oligonucleotides with polyamines

The polyamines (final concentration: 10 μM, unless stated otherwise) were added to the duplex oligonucleotides (final concentration: 0.2 μM) in 15 mM $KAsO_2Me_2$, 115 mM KCl, pH 6.5 buffer (unless stated otherwise; the pH of the buffer was adjusted using HCl or KOH solutions), and incubated at 37°C for the indicated amount of time. The reactions at pH 7.2 and 8.5 were performed in 15 mM HEPES, 115 mM KCl buffer. The reactions were terminated by addition of gel loading buffer (formamide, 0.05% bromophenol blue, 0.05% xylene cyanol). The samples were analyzed by gel electrophoresis in 20% polyacrylamide gels containing 8.3 M urea in 1X TBE buffer at 20 W for 3 h. Gels were exposed to phosphor imaging screens (Molecular Dynamics). After overnight exposure, the screens were scanned with Amersham Typhoon 5 Biomolecular Imager (GE Healthcare), quantified and analyzed using ImageQuant TL 8.2 software (GE Healthcare).

Enzymatic reactions

Human recombinant APE1 (Sino Biological) was rehydrated with milli-Q water at a concentration of 250 μg ml^{-1}, diluted with storage buffer (10 mM Tris–HCl, 50 mM NaCl, 0.05 mM Na_2EDTA, 1 mM DTT, 200 μg ml^{-1} BSA) to a concentration of 15 μg ml^{-1}, aliquoted and stored at –20°C. The AP-X adduct was prepared by incubation of the AP duplex (0.2 μM) and polyamines (10 μM) in 10 μl of reaction buffer (15 mM $KAsO_2Me_2$, 115 mM KCl, pH 6.5) for 3 h at 37°C. Then, APE1 (final concentration: 0.083 μg ml^{-1}, ∼2.3 nM) and $MgCl_2$ (final concentration: 1.7 mM) were added, and samples were additionally incubated at 37°C for 0 to 120 min. The untreated AP duplex was used as a control. The reactions were terminated by addition of gel loading buffer and analyzed by gel electrophoresis as described above.

Human recombinant TDP1 was expressed and purified as described elsewhere (65). AP-X adducts were prepared as described above in 50 mM Tris–HCl, 50 mM NaCl, 1 mM DTT, pH 8.5 buffer. Then, TDP1 (final concentration: 0.5 μM) was added and samples were additionally incubated at 37°C for 0 to 60 min. AP duplex and C12 duplex (3-T(C_{12})C/5-GTA) were used as control substrates to validate TDP1 activity.

LC/MS analysis of modified oligonucleotides

RP-UPLC/MS analyses were performed on a Waters Acquity system equipped with a SQ Detector 2. Analyses were performed on a Premier Oligonucleotide C_{18} Column (130 Å, 1.7 μm, 2.1 × 50 mm) using a linear gradient of 0 to 30% of solvent B (0.5% of HFIP + 0.2% TEA in Optima LC/MS MeOH) in solvent A (0.5% of HFIP + 0.2% TEA in milli-Q water) for 12 min at 50°C with UV detection at 260 nm unless otherwise specified. Mass detection was performed in the negative ionization mode with a 600–2000 Da mass range. Mass assignments from the mass spectra of the UV-detected peaks were performed by deconvolution of multiply charged MS data to the zero charge state using built-in Waters MaxEnt™ 1 software. Chromatograms were visualized and processed with MestReNova software.

Results and discussion

Structural determinants for reaction of polyamines with AP sites, fU and fC

Among the twelve naphthalenophanes whose reaction with AP sites was previously investigated, only BisNP-NH gave a clear formation of a covalent adduct, whereas trace amounts of the adduct were observed with BisNP-O (59). Considering this fact, in this work we systematically modified the chemical structure of polyamines in order to elucidate the structural features that govern this type of reactivity. Our panel (Figure 2A) included naphthalenophanes BisNP-NH and BisNP-O; a novel, hybrid naphthalenophane BisNP-NH/O combining polyamine and ether linkers (synthesis and characterization: Supplementary Scheme S1 and Supplementary Figure S1); three open-chain analogues featuring different number of secondary amino groups and/or carbon atoms between the two naphthalene moieties (BisNP-$\frac{1}{2}$, C2N2, and C33N3); two benzyl counterparts (DBDT and DBED); as well as three macrocyclic polyamines devoid of aromatic groups (TACN, cyclen, and hexacyclen). With this panel of eleven compounds, we set to investigate the influence of the presence and the size of aromatic units, as well as of the length and the number of amino groups in the linkers between these units, on the reactivity with AP sites and two other aldehyde-containing DNA modifications, fU and fC.

To study the reactivity of polyamines, 17-mer DNA oligonucleotides (Table 1) containing an aldehyde modification (fU or fC), dU as a precursor of the AP site, or unmodified control were 5′-^{32}P-labelled, hybridized to the complementary strand, and the AP site was generated by treatment of the dU duplex with uracil DNA glycosylase (UDG). The generation of AP site was systematically verified using 0.5 M NaOH treatment (25), evidencing of the absence of uncleaved, dU-containing strand (e.g. Figure 2B, lane 2). As the stability of AP sites decreases at pH > 7.5, the initial set of experiments was performed in slightly acidic conditions (pH 6.5) allowing further modulation of reactivity by either increasing or decreasing pH. The duplexes (0.2 μM) were made to react with polyamines (10 μM) in identical conditions (37°C, 3 h), and the products were analyzed by denaturing polyacrylamide gel electrophoresis (PAGE), visualized and quantified by phosphorimaging (Figure 2B–D). The reaction with the unmodified control duplex was also assessed, giving evidence of no reaction with any of polyamines (Supplementary Figure S2).

Reactivity towards AP sites. Polyamines containing aromatic units efficiently reacted with AP sites, leading to disappearance of the uncleaved AP strand and formation of various products, including the products of strand cleavage through β-elimination (3′-PUA and the closely migrating 3′-dR product, both labelled as 'β' in Figure 2B), β,δ-elimination (3′-P, 'δ'), and adducts of polyamines to the cleaved AP sites ('AP-X') that migrated in PAGE between the uncleaved strand and 'β' bands. Of note, the electrophoretic mobility of AP-X adducts depends on the nature of the polyamine remnant, with bulkier and more charged polyamines (e.g. BisNP-NH) giving more slowly migrating adducts and *vice versa*. BisNP-NH gave 25% of the AP-X adduct, which is somewhat less than in our previous work (59), presumably due to small differences in experimental conditions (reaction time, pH). BisNP-O effectively cleaved the AP site without formation of adducts (95% of β + δ-cleavage products), whereas the hybrid macrocycle BisNP-NH/O gave 19% yield of the adduct. This already indicates that the diethylenetriamine linker present in BisNP-NH and BisNP-NH/O is critical for the formation of the adducts, whereas the oxygen-containing linkers in BisNP-O are inactive in this regard. Remarkably, open-chain polyamines BisNP-$\frac{1}{2}$ and C2N2 produced significantly higher yields of AP-X adducts (85% and 74%, respectively), whereas the analogue C33N3 containing three carbon atoms between the adjacent amino groups (in contrast to two carbons in BisNP-$\frac{1}{2}$ and C2N2) produced <2% of the adduct, despite being very effective in terms of AP-site cleavage (97% of β + δ-cleavage products). Comparing with their naphthalene analogues, benzyl derivatives DBDT and DBED were much less reactive, as evidenced by the presence of significant amounts of the uncleaved AP strand (51–63%), and gave AP-X adducts with the yields of 10% and 15%, respectively. In contrast, macrocyclic polyamines devoid of aromatic units (TACN, cyclen and hexacyclen) were totally unreactive in these conditions, yielding neither adducts nor strand cleavage. Collectively, these results indicate that compound DBED, combining a secondary 1,2-diamine fragment with the presence of two benzyl groups, represents a minimal and sufficient motif for the formation of a covalent adduct upon reaction with cleaved AP sites, and that replacement of benzyl groups with naphthalene counterparts (as in C2N2) leads to a dramatic enhancement of both AP site cleavage efficiency and the yield of AP-X adducts. This effect most likely stems from the higher non-covalent DNA affinity of naphthalene derivatives due to intercalation of naphthalene moieties, resulting in an increased local concentration of the reagent (66). To illustrate this point, we tested the reaction of the AP duplex with a ten-fold higher concentration of DBED (i.e. 100 μM) and observed an increase of adduct yield up to 48% (Supplementary Figure S3A), which indicates that adduct yield indeed depends on the polyamine concentration.

Reactivity towards fU and fC. Upon reaction with fU duplex, several polyamines gave rise to the formation of covalent adducts without cleavage of DNA strands, evidenced as bands migrating in PAGE slower than the unreacted strand (fU-X, Figure 2C). Remarkably, naphthalenophanes BisNP-NH and BisNP-NH/O gave higher yield of adducts upon reaction with fU than with AP sites (BisNP-NH: 39% fU-X vs. 25% AP-X; BisNP-NH/O: 24% fU-X vs. 19% AP-X). In the case of open-chain analogues, this tendency was inverse (BisNP-$\frac{1}{2}$: 25% fU-X vs. 85% AP-X; C2N2: 7% fU-X vs. 74% AP-X). Benzyl analogues DBDT and DBED gave only traces (<5%) of the corresponding adducts; however, in the case of DBED, the adduct yield could be increased up to 12% by raising the reagent concentration from 10 to 100 μM (Supplementary Figure S3B). Conversely, naphthalenophane BisNP-O, as well as C33N3 and polyamines devoid of aromatic units, did not form any adducts. Altogether, these observations suggest that, upon reaction with fU, the secondary 1,2-diamine fragment is also the critical structural determinant for adduct formation; in addition—and different to the AP-site reactivity—the macrocyclic scaffold acts as an efficient reactivity enhancer.

Similarly to the reaction with fU, bis-naphthalenes BisNP-NH and BisNP-NH/O, as well as open-chain analogues BisNP-$\frac{1}{2}$ and C2N2, gave rise to the formation of adducts upon reaction with fC residues, observed as bands migrating in PAGE slower that unreacted strands (fC-X, Figure 2D). However, the efficiency of this reaction was much lower, with the adduct yield not exceeding 5–6%.

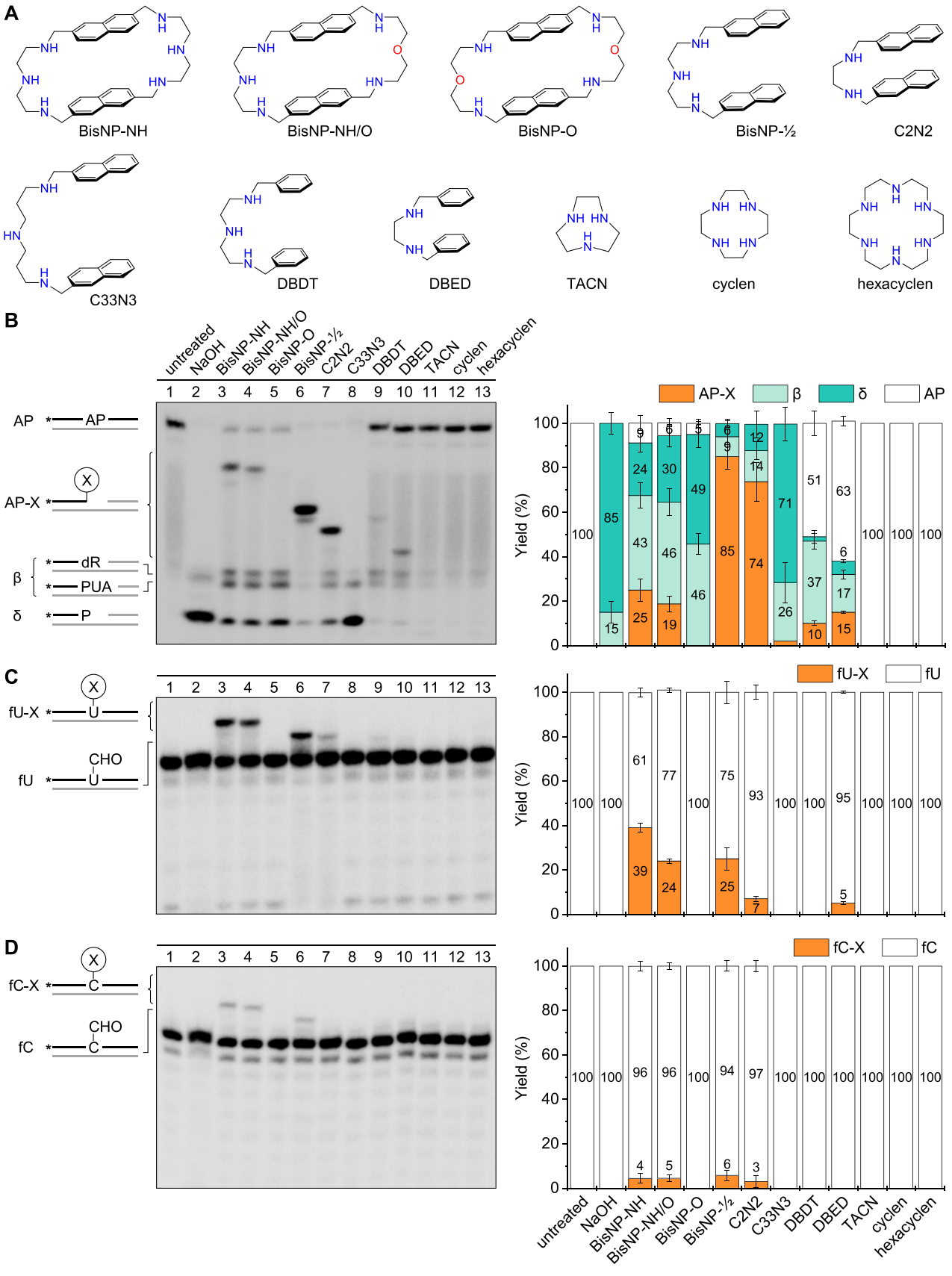

Figure 2. (**A**) Chemical structures of polyamines investigated in this study. (**B**–**D**) Representative PAGE analysis (left) and quantification of products (right, means ± s.d., $N \geq 3$) obtained in reactions of polyamines with DNA duplexes containing (**B**) AP site, (**C**) fU and (**D**) fC residues. The structures of products are schematically shown left to PAGE gels, where * is a ^{32}P label and X a polyamine remnant. Conditions: 0.2 μM duplex substrate, 10 μM polyamine in 15 mM $KAsO_2Me_2$ and 115 mM KCl buffer, pH 6.5, temperature: 37°C, reaction time: 3 h.

Chemical structure of AP-X adducts and reaction mechanism

In order to elucidate the structures of the adducts formed upon reaction of AP sites with polyamines, we studied the reaction of 5-*O*-TBDPS-3-*O*-acetyl-2-deoxyribofuranose **1**, representing an accurate small-molecule mimic of uncleaved AP site, and 5-*O*-TBDPS-4,5-dihydroxypent-2-enal **2**, representing a mimic of the 3′-PUA residue (63), with DBED as the structurally simplest compound that still demonstrates this type of reactivity (cf. Supplementary Figure S3A). Upon reaction of equimolar amounts of DBED acetate and either **1** and **2** in the conditions similar to those employed for DNA oligonucleotides, we observed the formation of two isomeric products, that could be isolated and were identified as diastereomers **3α** and **3β**, containing the same tetrahydrofuro[2,3,4-*ef*]-1,4-diazepane (hereafter 'ribodiazepane') scaffold (Scheme 1). Remarkably, in both cases the diastereomeric ratio of the products was nearly identical, with α-diastereomer being largely predominant (**3α**:**3β** ≈ 95:5, as per HPLC analysis). When the reaction of DBED with **2** was performed in the presence of 2 molar equiv. of K_2CO_3 the diastereoselectivity of the reaction was reduced (**3α**:**3β** = 88:12, total yield: 83%), allowing to isolate pure samples of both diastereomers.

The structures of **3α** and **3β** were assigned on the basis of their 1D and 2D $^1H/^{13}C$ NMR and mass spectrometry data (Supplementary Figures S4–S9). In particular, the dissymmetry of benzyl groups and of the ethylenediamine bridge observed in ^1H NMR spectrum, along with the absence of characteristic aminal signals, strongly speaks against a putative 1,3-aminal structure, despite the well-known capacity of DBED to give 1,3-aminals upon reaction with various aliphatic and aromatic aldehydes (67–69). Instead, ^1H signals observed as doublets at δ = 5.02 (**3α**) and 5.01 ppm (**3β**) could be attributed to the anomeric protons (H^1) suggesting the presence of a deoxyribose remnant. The precise assignment of α- and β-diastereomers was performed through NOE difference spectra (Figure 3) obtained by selective irradiation of H^4 protons and considering the characteristic NOE couplings with regard to molecular models (Supplementary Note 1 and Figure S10), in particular the couplings between H^4 and the two protons of the ethylenediamine bridge (in **3α**) and between H^4 and H^1 (in **3β**).

To confirm that similar products were formed upon reaction with oligonucleotides, we analyzed by RP-UPLC/MS the reactions of AP duplex with C2N2 (Figure 4) and BisNP-$\frac{1}{2}$ (Supplementary Figure S11). In addition to the products of AP site cleavage (3′-P, 3′-dR and 5′-P) and the unmodified complementary strand, we observed the formation of products that were significantly retained in RP-UPLC (t_R ≈ 11.3 min), with *m*/*z* values consistent with the structures of the expected ribodiazepane adducts (*M* = 2941 and 2984 Da for and C2N2 and BisNP-$\frac{1}{2}$ adducts, respectively).

The mechanism proposed for the formation of 3′-ribodiazepane adducts upon reaction of polyamines with AP sites, 3′-PUA, or their small-molecule mimics is shown in Scheme 2. After formation of iminium intermediate **4** through the reaction of one of the secondary amino groups with the open-chain aldehyde (AP or **1**), the second amino group acts as internal base, efficiently inducing E2-type β-elimination of the leaving group X (OAc in **1**, or 5′-P in AP DNA) and leading to the formation of protonated α,β-unsaturated iminium **5**–H^+. The same compound **5** can be formed upon reaction of the diamine with α,β-unsaturated aldehyde (3′-PUA or **2**). After rotation about the single bond, iminium **5** (in *s-cis* conformation) undergoes intramolecular conjugate addition of the neighboring amino group. This aza-Michael-type addition can take place from the two enantiotopic faces of the unsaturated imine, either from the *re* face leading to the formation of seven-membered cyclic enamine **6β** or preferentially, after rotation about the C−N bond, from the *si* face leading to the formation of cyclic enamine **6α**. Enamines **6α/β** undergo reversible protonation at their α-carbons, following by internal nucleophilic attack of the hydroxyl group at the iminium center (in both cases, *anti*-periplanar with respect to the amino group at C3), leading to the closure of the ribose ring and, after deprotonation, formation of ribodiazepanes **3α/β**.

Although conjugate addition of *N*- and *S*-nucleophiles to iminium intermediates such as **5** is well-documented (25,34,63) and, presumably, is involved in the formation of certain DPCs (30,31,33) and DNA ICLs from 3′-PUA (26,27), the formation of bicyclic ribodiazepane-type adducts is unprecedented. Gates et al. recently investigated the reaction of the AP-site mimic **1** with *N,N*′-dimethylethylenediamine (DMEDA), structurally very close to DBED (cf. Supplementary Figure S3), but failed to observe any stable adducts; instead, they observed the formation of 5-*O*-TBDPS-2-deoxyribose **7** (Scheme 2), resulting from conjugate addition of water to iminium intermediate **5** (R = CH_3) followed by hydrolysis of the enamine (63). In light of that study, we reassessed the reaction of **1** and AP duplex with DMEDA. Upon reaction of equimolar amounts of **1** and DMEDA in neutral conditions (acetonitrile/phosphate buffer 9:1, pH 7.0) we observed the formation of dimethyl-ribodiazepane **8α** as a predominant diastereomer, that was isolated in a 46% yield and fully characterized (Supplementary Scheme S2 and Figures S12–S13). Of note, using the conditions previously reported by Gates et al. (10 mol % DMEDA in acetonitrile / 10 mM aq. NaOH 1:1, 37°C, 14 h), we observed poor conversion of **1** and only trace amounts of deoxyribose **7**, along with ribodiazepane **8α**, could be detected by HPLC analysis (Supporting Information, Figure S14). However, the reaction of DMEDA with AP duplex in the same conditions as employed for other polyamines did not produce any adduct, even upon increasing the concentration of DMEDA up to 100 μM (Supplementary Figure S3C). This implies that the role of aromatic groups in DBED (and other polyamines used in our study) resides in enhancement of DNA binding of polyamines by π-stacking with nucleobases (i.e. intercalation), leading to a dramatic increase of effective concentration at the reaction site. In agreement with this hypothesis, naphthalene derivatives with larger π-surface area are systematically more reactive than benzyl analogues (cf. Figure 2B).

Interestingly, Greenberg et al. observed the formation of the cyclic 1,4-diazepan-5-one product upon reaction of very high concentrations of DMEDA (0.1 M) with oxidized (2-deoxyribonolactone) abasic sites (Supplementary Scheme S3A); however, the lactam nature of this product does not permit the intramolecular addition of the 4-hydroxyl group that would result in formation of a bicyclic structure (70). Finally, we note that Román *et al.* observed the formation of a bicyclic derivative upon reaction of 3,6-anhydro-2-deoxy-D-glycose with 1,2-phenylenediamine (Supplementary Scheme S3B); this example is most closely related to ribodiazepanes described here (71).

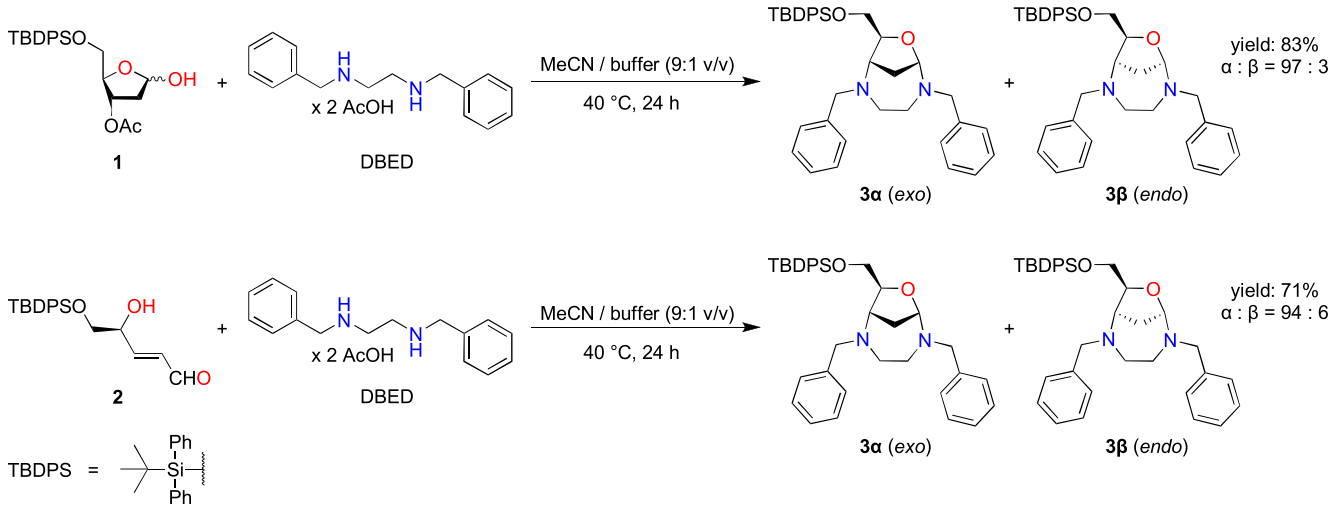

Scheme 1. Reactions of DBED acetate with small-molecule mimics of AP site (**1**) and 3′-PUA (**2**).

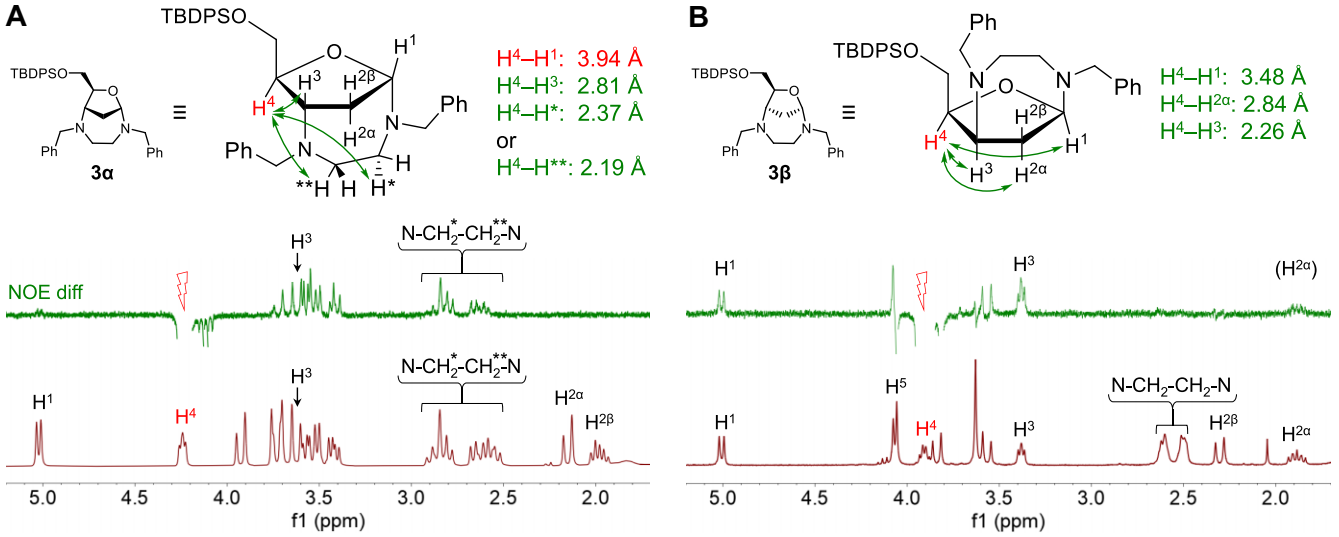

Figure 3. Structures of **3**α (**A**) and **3**β (**B**) indicating selected interatomic distances (according to molecular models, cf. Supplementary Figure S16) and observed NOE couplings (green arrows). In **3**α, two clusters of conformations were observed differing by the pucker of the ethylenediamine bridge and the proximity of either H* or H** to H^4 (cf. Supplementary Note 1). Bottom panels: ^{1}H NMR (300 MHz, $CDCl_3$, dark red) and 1D NOE difference spectra (green) obtained by selective irradiation of H^4 protons.

Chemical structure of fU-X adducts and reaction mechanism

To elucidate the structure of the adducts formed in reaction of polyamines with fU residues, we studied the reaction of DBED with 1-methyl-5-formyluracil (1-Me-fU). The conversion of this substrate required significantly longer time (3 days at 40°C), which is consistent with lower reactivity of DBED towards fU comparing with AP sites (cf. Supplementary Figure S3A, B). After purification by semi-preparative HPLC and ion exchange (aq. HBr), we successfully isolated a single product that was identified as 1,4-dibenzyl-6-(*N*′-methylallophanyl)-2,3-dihydro-1,4-diazepinium bromide **9** (Scheme 3).

The structure of **9** was assigned on the basis of its ^{1}H and ^{13}C NMR spectra and mass spectrometry (Supplementary Figures S15–S17). In particular, ^{1}H NMR spectrum (Figure 5A) indicated a symmetry of the two benzyl groups, a broad signal for the ethylenediamine bridge, along with a strongly deshielded singlet signal of two chemically equivalent protons (δ = 8.55 ppm). These features are characteristic of cationic 2,3-dihydro-1,4-diazepiniums (72,73). Additionally, the UV spectrum of **9** (Figure 5B) featured an absorption band at λ = 336 nm, which is also characteristic for 2,3-dihydro-1,4-diazepiniums due to the presence of a vinamidinium, or 'streptocyanine' π-conjugated system (74,75).

The characteristic UV absorption of the diazepinium fragment can be employed for the detection of fU-X adducts upon reaction of polyamines with fU-containing oligonucleotides. Towards this end, we reacted fU duplex with BisNP-NH (as the polyamine giving the highest yield of the fU-X adduct) and monitored the reaction by UV spectrophotometry. We

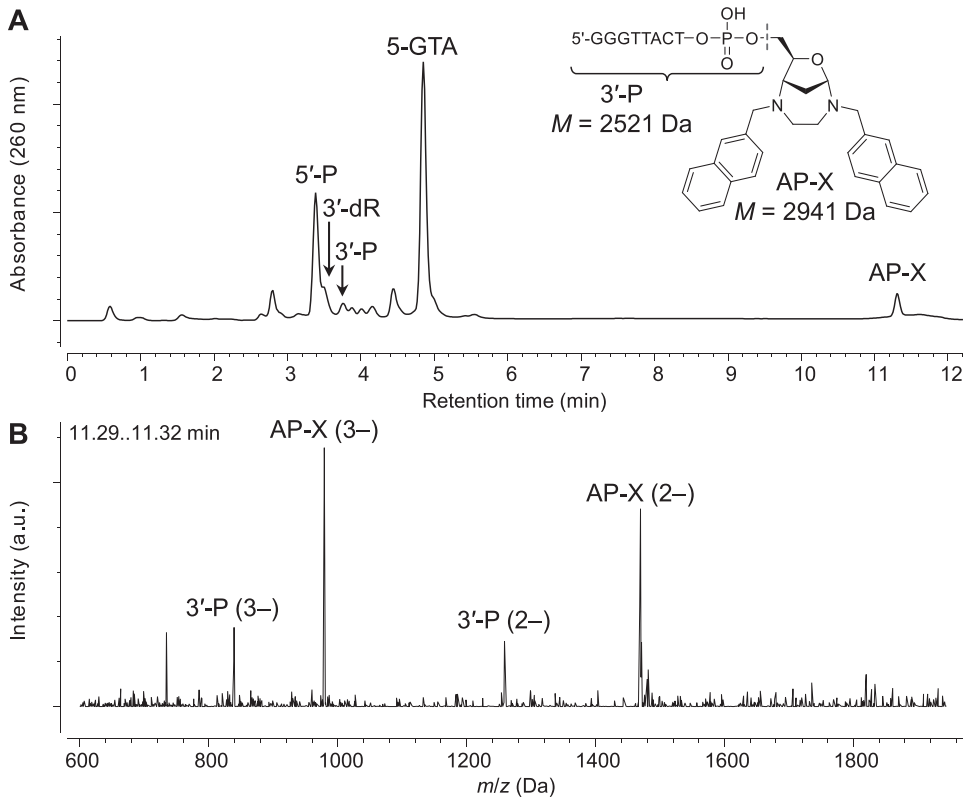

Figure 4. (**A**) UV-UPLC analysis of products obtained upon reaction of AP duplex (20 μM) with C2N2 (40 μM) in 15 mM $KAsO_2Me_2$, 115 mM KCl, pH 6.5 buffer. Whenever possible, the peaks were assigned on the basis of their mass spectra. (**B**) Mass spectrum (ESI$^-$) of the UPLC peak with t_R = 11.30 min (AP-X). The peaks attributed to 3′-P presumably arise from fragmentation of AP-X, shown by the dashed line in panel (A).

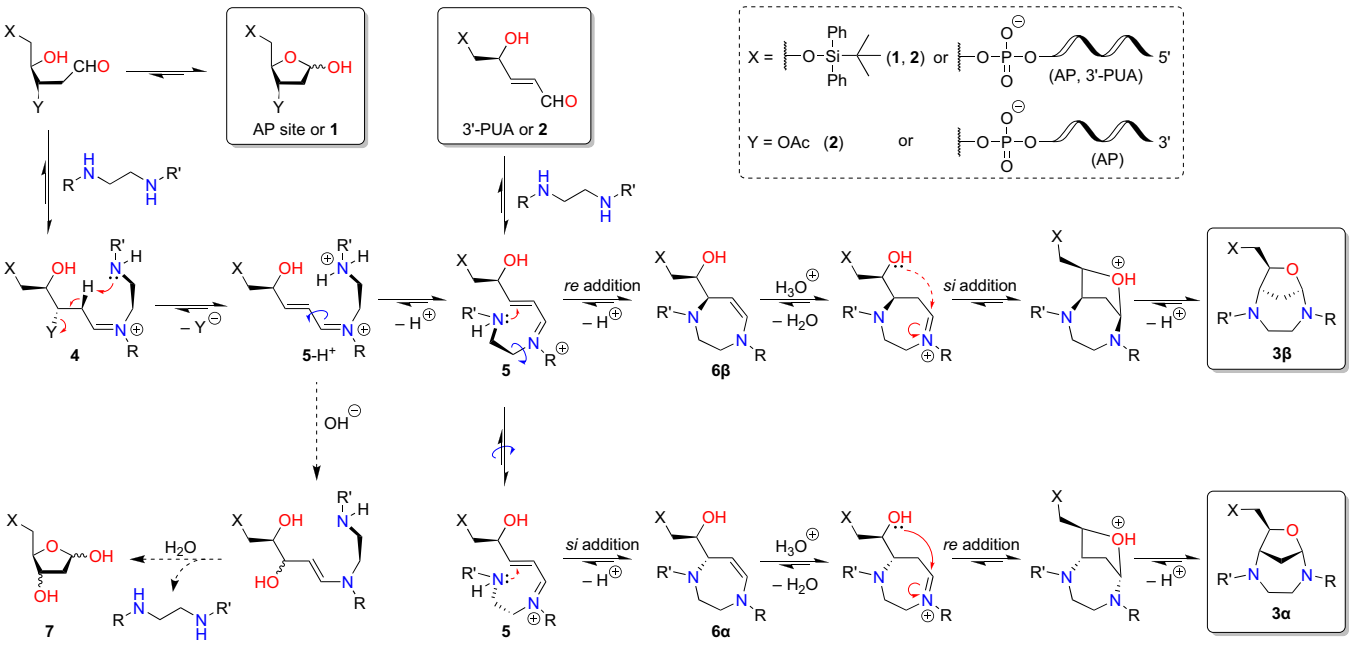

Scheme 2. Proposed mechanism of formation of 'ribodiazepane' adducts upon reaction of secondary polyamines with AP sites, 3′-PUA, or their small-molecule analogues. The dashed arrows show the reactions observed by Gates *et al.* (63).

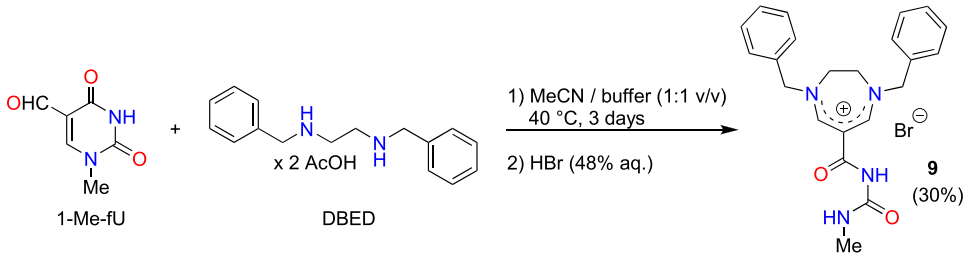

Scheme 3. Reaction of DBED acetate with 1-methyl-5-formyluracil (1-Me-fU).

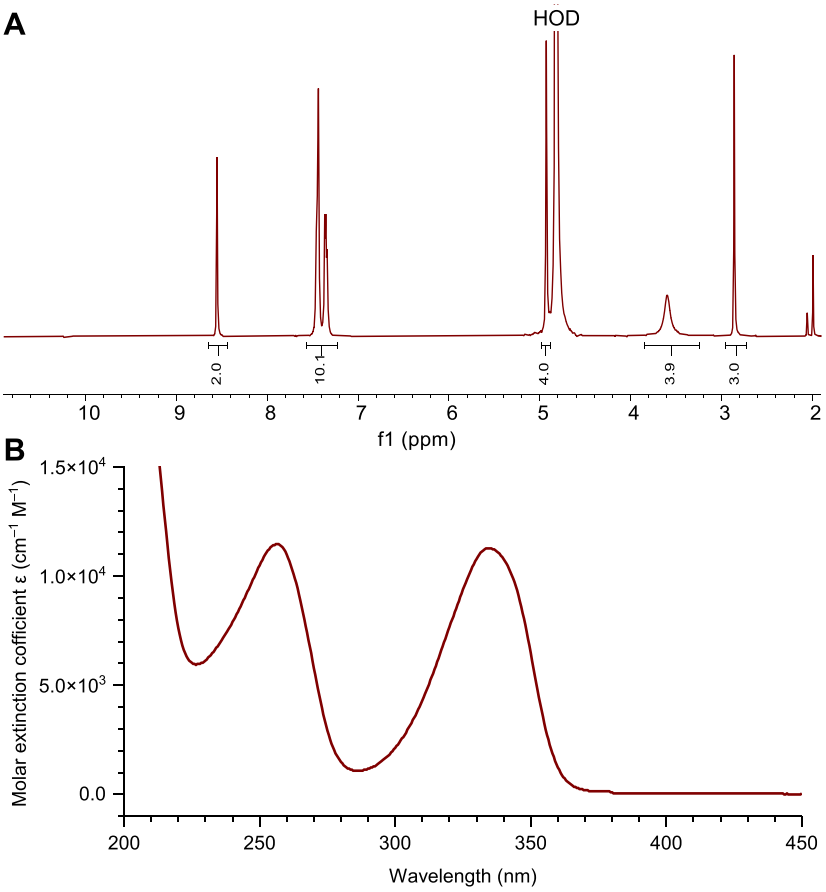

Figure 5. (**A**) ^{1}H NMR (D_2O, 300 MHz) and (**B**) UV spectra (H_2O, $c = 20$ μM) of compound **9**.

observed a time-dependent appearance of a characteristic absorption peak at $\lambda \approx 340$ nm, giving evidence that the reaction reached an equilibrium after ∼10 h (Figure 6A, B). Moreover, the reaction of the fU-modified single-stranded oligonucleotide 3-(fU)AC with BisNP-NH was additionally analyzed by LC/MS, giving evidence of the presence of two major peaks (Figure 6C), namely the unreacted oligonucleotide and the fU-X product with higher retention time ($t_R = 6.50$ min), that could be selectively detected by absorption at 340 nm (Figure 6D). Satisfyingly, the mass spectrum of the fU-X peak (Figure 6E) was found in full agreement with the formation of the diazepinium adduct (shown as inset in Figure 6C).

The putative mechanism for the formation of diazepinium adducts is shown in Scheme 4. After the initial formation of iminium intermediate upon reaction of the aldehyde group of fU with one of the secondary amino groups of the 1,2-diamine fragment, the second amino group undergoes an aza-Michael addition to C-6 of the uracil, resulting in the formation of enamine intermediate **10**. Similar to the reaction with AP sites, the enamine is protonated at its α-carbon atom (i.e. C-5 of the uracil), followed by ring-opening of the uracil with elimination of the urea fragment and formation of the 2,3-dihydro-1,4-diazepinium system **9**. The ring-opening reactions upon addition of *N*- and *C*-nucleophiles at C-6 of uracil are well described in the literature (76–80). Moreover, Sochacka & Smuga observed ring-opening of fU with formation of acyclic vinamidines upon reaction of fU with primary amines (81). However, the formation of 1,4-diazepinium adducts described here is unprecedented, as it can occur only with secondary 1,2-diamines.

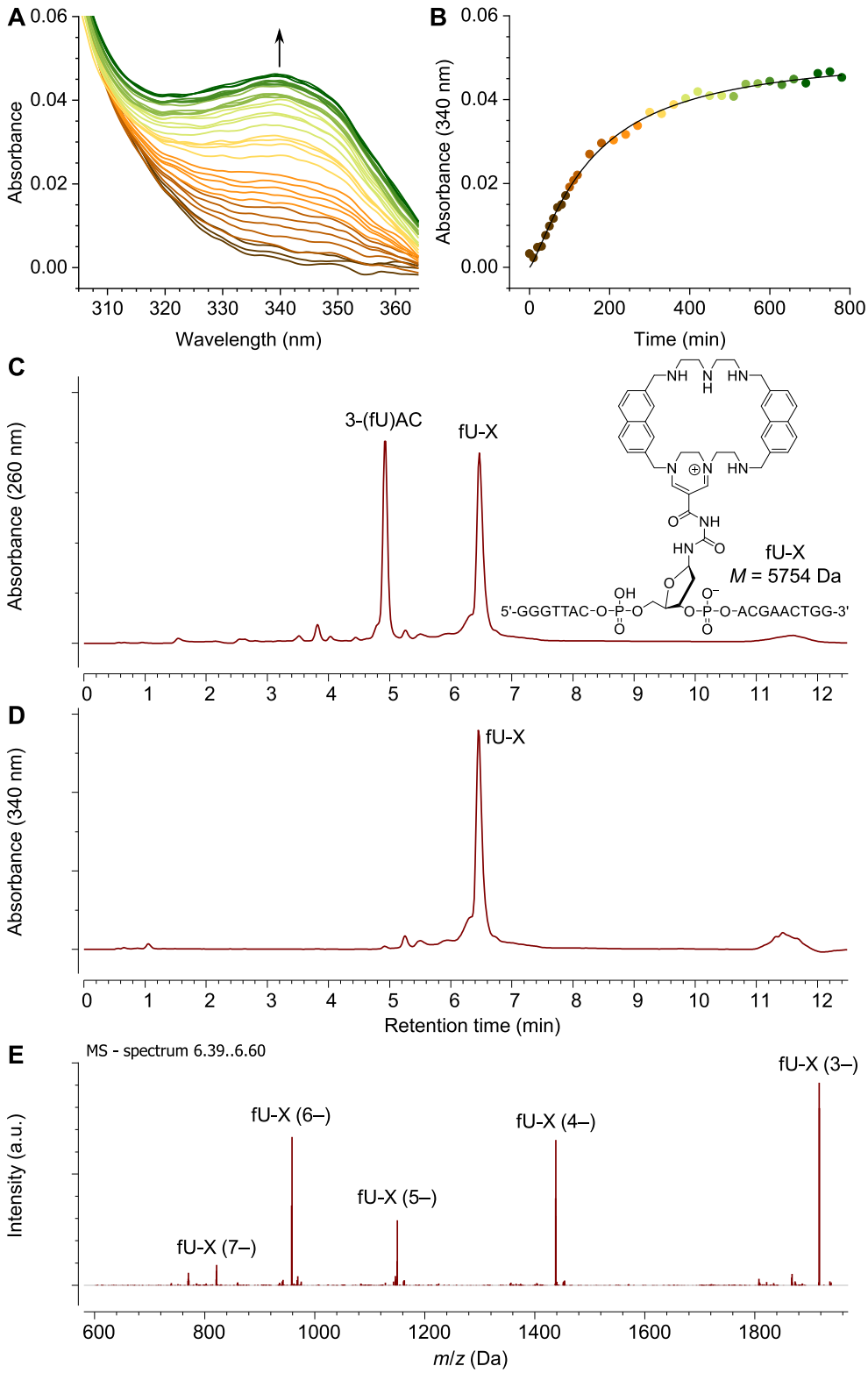

Figure 6. (**A**–**B**) Changes of in absorption spectra (**A**) and time course (**B**) of the reaction of fU duplex (3-(fU)AC/5-GTA, 10 μM) with BisNP-NH (20 μM) in 15 mM $KAsO_2Me_2$, 115 mM KCl buffer, pH 7.2, reaction temperature: 37°C. (**C**–**D**) UV-UPLC analysis of reaction of the fU-containing strand 3-(fU)AC (20 μM) with BisNP-NH (40 μM) performed in the conditions described above, detected at the wavelengths of 260 nm (**C**) and 340 nm (**D**). (**E**) Mass spectrum (ESI^-) of the UPLC peak with $t_R = 6.50$ min (fU-X). The putative structure of the fU-X adduct is shown as inset in (**C**).

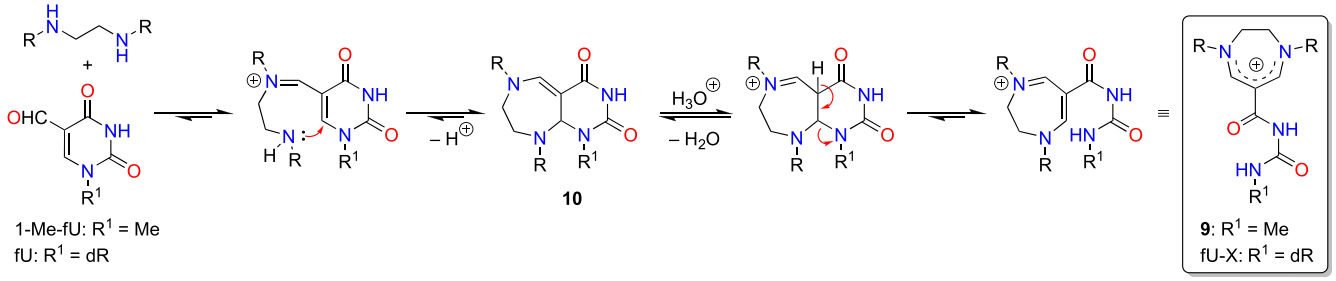

Scheme 4. Proposed mechanism of formation of 6-allophanyl-2,3-dihydro-1,4-diazepinium adducts upon reaction of secondary polyamines with 5-formyluracil derivatives. R is as in Scheme 3.

Influence of reaction conditions on adduct yields and chemoselectivity of polyamines

To determine whether the yield of DNA–polyamine adducts could be further improved, we systematically investigated the influence of several parameters on the reaction of the three most reactive polyamines (BisNP-NH, BisNP-$\frac{1}{2}$, and C2N2) with AP-, fU- and fC duplexes. First, as it was already observed for DBED (cf. Supplementary Figure S3A,B), the yield of adducts was found to depend on the polyamine concentration (Figure 7A–C): while no adducts were detected at polyamine concentrations of 0.1 μM, AP-X and fU-X adducts could be detected at polyamine concentrations as low as 0.5–1 μM. In most cases, the adduct yield was significantly higher at 5 μM of polyamine; this is particularly spectacular for the reaction of AP sites with BisNP-$\frac{1}{2}$ and C2N2, which gave over 80% yield of AP-X adducts at 5–10 μM. Interestingly, the relative reactivity of the three polyamines with respect to AP, fU and fC substrates was different, but the reactivity order was mostly maintained in the whole range of concentrations (AP: BisNP-$\frac{1}{2}$ > C2N2 > BisNP-NH; fU: BisNP-NH > BisNP-$\frac{1}{2}$ >> C2N2; fC: BisNP-$\frac{1}{2}$ ≥ BisNP-NH >> C2N2). This indicates that the structure of the polyamine determines its preferential reactivity with one or another substrate.

Next, we studied the effect of reaction pH, in the 5.0–8.5 range, on the yield of polyamine adducts (Figure 7D–F). In the reaction with AP sites, the yields of all three adducts gradually increased upon rising pH from 5.0 to 8.5 (Figure 7D), with a particularly sharp increase observed for BisNP-NH in the pH range 6.5–7.8 (from 23% to 73%, i.e. 3.1-fold); BisNP-$\frac{1}{2}$ and C2N2 gave nearly quantitative yield of AP-X (> 90%) in neutral to slightly basic conditions (pH 7.2–8.5). In the reaction with fU, the yield of BisNP-NH adduct also increased upon rising pH (from 12% at pH 5.0 to 55–60% at pH 7.2 and above), whereas a two-fold *decrease* was observed for BisNP-$\frac{1}{2}$ (from 30% to ∼15%). Finally, the yield of fC-X adducts increased upon raising pH for all three compounds, but remained low (≤ 10%) even in most basic conditions (pH 8.5, Figure 7F). Altogether, these results provide interesting clues with regard to chemoselectivity of polyamines, quantified as a ratio of yields of the corresponding adducts (Figure 7G, H). Thus, BisNP-NH shows highest chemoselectivity for fU over AP sites at pH 6.5 (AP-X/fU-X ≈ 0.5); in contrast, the chemoselectivity of BisNP-$\frac{1}{2}$ and C2N2 for AP sites versus fU is highest in neutral conditions (AP-X / fU-X = 5.5 and ∼20, respectively, at pH 7.2), and their chemoselectivity with respect to fC increases at low pH values (AP-X/fC-X = 23 and 72, respectively, at pH 5.0). Collectively, these data suggest that C2N2 is the preferred reagent for labeling of AP sites, allowing to achieve satisfactory chemoselectivity (∼20-fold) with respect to both fU and fC at physiological pH 7.2.

Finally, we studied the reaction kinetics of AP and fU duplexes with BisNP-$\frac{1}{2}$ at two temperatures, 20°C and 37°C (Figure 7I, Supplementary Figure S21). The yields of fU-X and, in particular, AP-X adducts was systematically higher at 37°C and reached plateaus after ∼1 h at this temperature. At 20°C, the reaction with the fU duplex also reached a plateau after ∼1 h, whereas the reaction with the AP duplex was incomplete even after 3 h, suggesting a slower kinetics.

Reactivity of polyamines with AP sites and fU in the presence of excess genomic DNA

We investigated whether the reaction of polyamines with AP sites and/or fU residues could be affected by the presence of undamaged genomic DNA. Although chemically inert, undamaged double-stranded DNA could sequester the cationic polyamines via non-covalent, reversible binding, decreasing their effective concentration and reducing the efficiency of adduct formation. We performed the reaction of AP duplex with increasing concentrations of BisNP-NH, BisNP-$\frac{1}{2}$ and C2N2 (10–100 μM) in the absence and in the presence of calf thymus (ct) DNA at concentrations of 0.2 and 2 mM base pairs (bp), i.e. in 1000- and 10 000-fold molar excess with respect to AP substrate. Interestingly, the yield of the BisNP-NH adduct did not decrease, but *increased* in the presence of ct DNA, reaching ∼65% in the presence of 2 mM ct DNA and 100 μM BisNP-NH (Figure 8A). The strong affinity of BisNP-NH (and related macrocyclic polyamines) to AP sites and lack of interaction with undamaged double-stranded DNA (58,59) could explain the persistence of adduct yield despite the presence of large excess of ct DNA; however, the reasons for the observed increase of the yield are unclear. Conversely, the yields of BisNP-$\frac{1}{2}$ and C2N2 adducts significantly decreased in the presence of ct DNA; satisfyingly, this effect could be mitigated by increasing the polyamine concentration to 50–100 μM, allowing to restore the AP-X yield to ∼70% in the presence of 2 mM bp ct DNA (Figure 8B, C).

The effect of ct DNA on the reaction of fU duplex with BisNP-NH was also investigated. In this case, the presence of 2 mM bp ct DNA decreased of the yield of fU-X adduct almost 2-fold (from 46% to ∼24%) when 10 μM BisNP-NH was used. Again, this effect could be countered by increasing the concentration of the reagent to 100 μM, allowing to reach the fU-X yield of 63% (Figure 8D). This behavior is suggestive of lower non-covalent affinity of BisNP-NH for fU sites comparing with AP sites (as a prerequisite for covalent reaction),

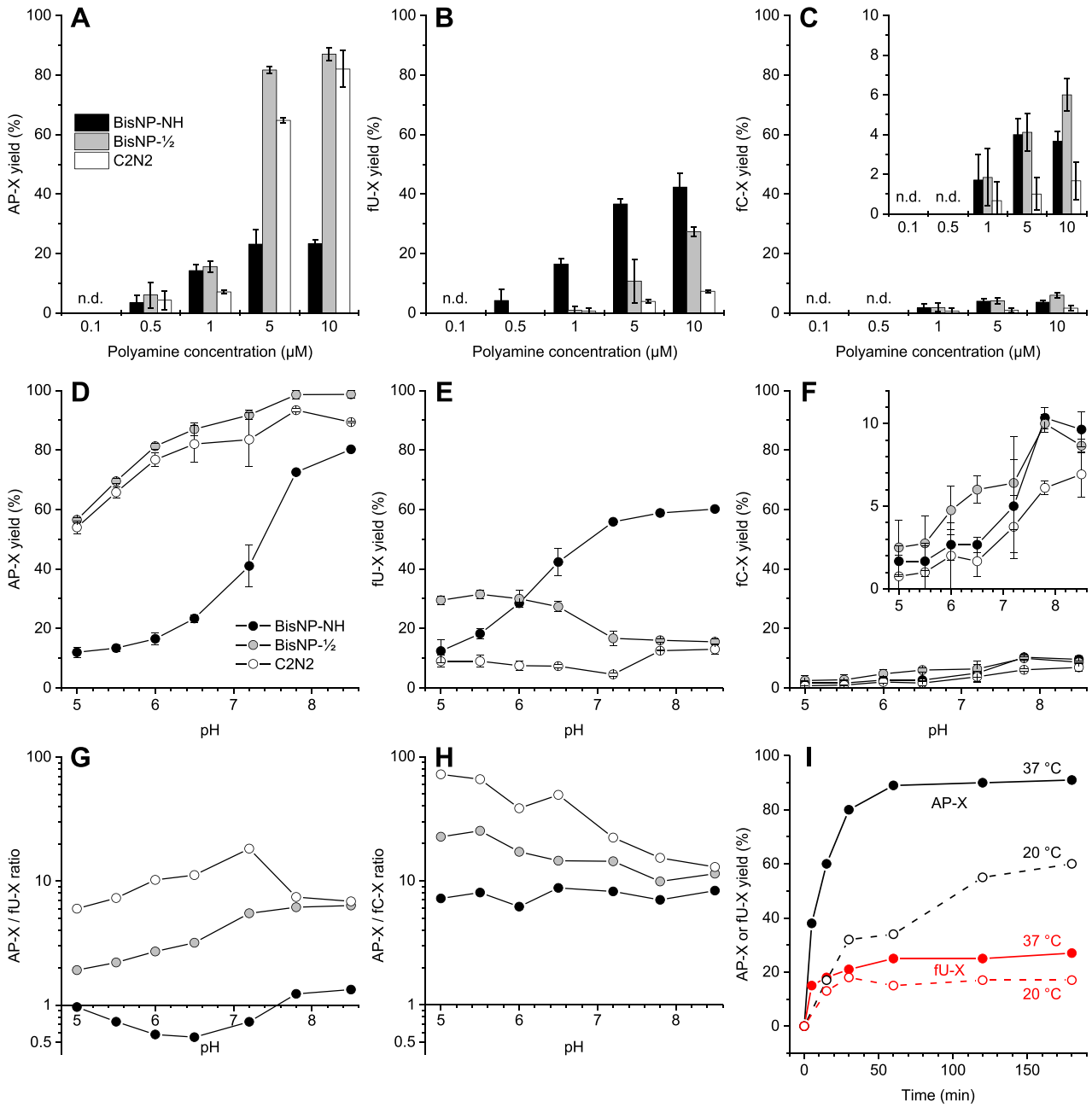

Figure 7. (**A**–**F**) Influence of polyamine concentration (**A**–**B**) and pH (**D**–**F**) on the yield of adducts formed upon reaction of BisNP-NH (black), BisNP-$\frac{1}{2}$ (grey) and C2N2 (white) with AP (**A**,**D**), fU (**B**,**E**) and fC (**C**,**F**) duplexes, as determined by quantification of denaturing PAGE data (cf. Supplementary Figures S18–S20). In (**A**–**C**), the reaction pH was 6.5. In (**D**–**F**), the polyamine concentration was 10 μM. All other conditions were identical: 0.2 μM substrate in 15 mM $KAsO_2Me_2$ (or 15 mM HEPES for pH > 7.2), 115 mM KCl buffer; reaction time, 3 h; temperature, 37°C. Data are means ± s.d. from three or more independent experiments; n.d. = not detected. (**G**–**H**) Ratio of AP-X to fU-X (**G**) or fC-X (**H**) adducts observed at different pH, calculated from the data in panels **D**–**F**. (**I**) Time dependence of the yield of AP-X (black) or fU-X adducts (red) in reactions of BisNP-$\frac{1}{2}$ (10 μM) with AP and fU duplexes at 37°C (filled dots and solid lines) and 20°C (empty dots and dashed lines), pH 6.5, other conditions as above (PAGE data: cf. Supplementary Figure S21).

resulting in a partial sequestration of the polyamine by the large excess of non-reactive ct DNA competitor.

Finally, we analyzed the yields of AP-X and fU-X adducts formed in reactions of polyamines with an equimolar mixture of AP and fU duplexes, in the absence and in the presence of ct DNA (Figure 9; cf. Supplementary Note 2 and Supplementary Table S1). The selectivity of polyamines observed in this competition experiment was globally in agreement with the reactivity profiles described above. In the absence of ct DNA, BisNP-NH gave predominantly fU-X adducts (26–30% AP-X vs. 70–73% fU-X, respectively); however, this ratio was skewed in favor of AP-X in the presence of ct DNA (e.g. 31% AP-X vs. 6% fU-X in the presence of 2 mM ct DNA and 10 μM BisNP-NH). Conversely, BisNP-$\frac{1}{2}$ and C2N2 systematically demonstrated preferential reactivity with AP substrate. Especially in the case of C2N2 (100 or 200 μM), the presence of ct DNA reduced the yield of fU-X adduct from 9–12% (in the absence of ct DNA) to 3–4% (2 mM ct DNA), whereas the

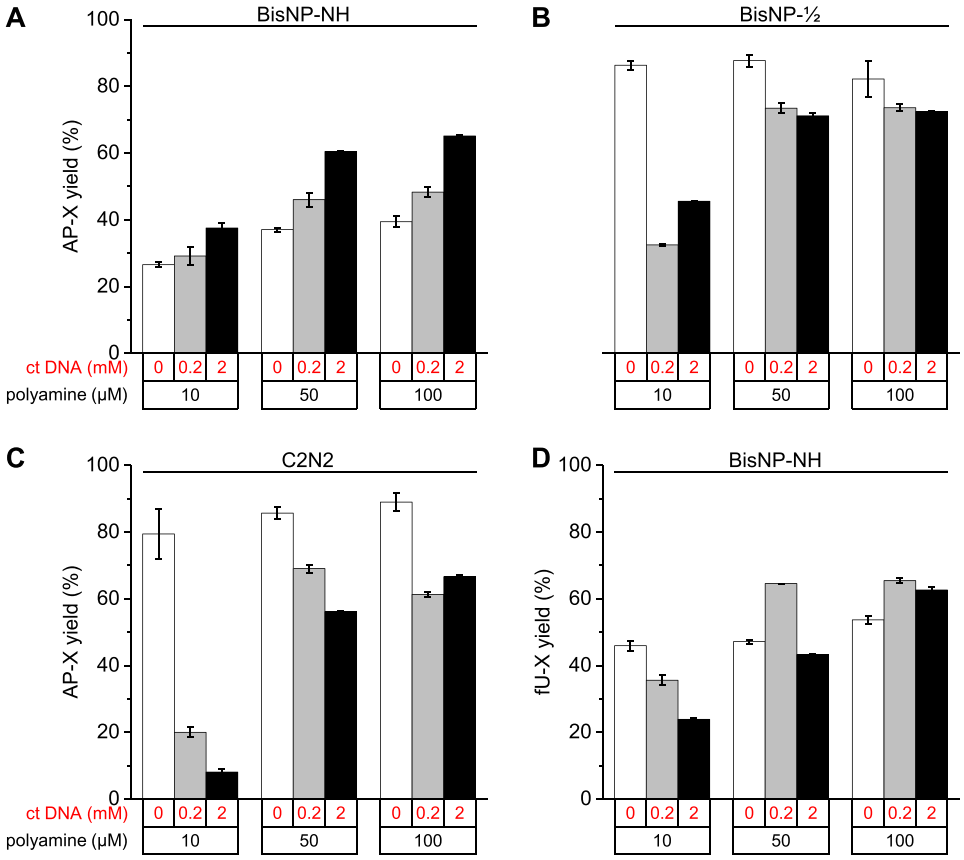

Figure 8. (**A**–**C**) Yield of AP-X adducts upon reaction of AP duplex with BisNP-NH (**A**), BisNP$\frac{1}{2}$ (**B**) and C2N2 (**C**) in the absence and in the presence of ct DNA (0.2 and 2 mM bp), as determined by quantification of denaturing PAGE data. (**D**) Yields of fU-X adducts upon reaction of fU duplex with BisNP-NH in the absence and in the presence of ct DNA (0.2 and 2 mM bp). Conditions: 0.2 μM substrate in 15 mM $KAsO_2Me_2$, 115 mM KCl buffer, pH 6.5; reaction time, 3 h, temperature, 37°C. Data are means ± s.d. from two independent experiments (cf. Supplementary Figure S22).

yield of the AP-X adduct was only slightly reduced (from 73–77% to ∼60%), giving evidence of a 15–20-fold selectivity for AP sites. Even if these conditions are less stringent comparing with the cellular environment (where the levels of AP sites and fU are estimated as ∼2 and ∼5 per 10^6 undamaged base pairs, respectively) (46,50), it demonstrates that BisNP-$\frac{1}{2}$ and, especially, C2N2 can efficiently and selectively label AP sites in the presence of both fU competitor and excess double-stranded DNA.

Chemical stability of AP-X and fU-X adducts

To evaluate the practical utility of polyamine adducts as chemical tools for labelling DNA modifications, we studied their stability with respect to several chemical reagents. Towards this end, AP-X adducts were prepared by treatment of the ^{32}P-labelled AP duplex with BisNP-NH, BisNP-$\frac{1}{2}$ or C2N2 in the conditions similar to the ones employed above (10 μM polyamine, 3 h, 37°C) and subsequently incubated for 25 min at 37°C in the presence of 0.1 M NaOH, 0.1 M HCl, 0.01 M $NaBH_4$, 0.01 M tris(2-carboxyethyl)phosphine (TCEP, reducing agent), or 0.1 M dithiothreitol (DTT, reducing agent and strong nucleophile), followed by PAGE analysis. The results (Figure 10A) indicate that the adducts were mostly stable in these conditions, as evidenced by the persistence of the corresponding AP-X bands. Incubation of the BisNP-NH adduct in the presence of DTT led to appearance of a novel band (* in Figure 10A), presumably corresponding to a thio-ddR adduct (25) that is formed upon reaction of DTT with 3′-PUA or iminium intermediates (cf. Scheme 2), and incubation in the presence of TCEP led to appearance of minor novel, fast-migrating bands (** in Figure 10A). TCEP is generally considered as a poor nucleophile; however, its addition reactions with strong Michael acceptors were recently documented (82), suggesting that, similar to DTT, it could form adducts upon reaction with 3′-PUA or the iminium intermediate. The putative TCEP adduct is expected to migrate fast in PAGE due to the presence of additional carboxylate groups. Remarkably, treatment of AP-X adducts with $NaBH_4$ resulted in the appearance of novel bands (*** in Figure 10A), migrating above the respective AP-X bands that were slightly reduced (BisNP-NH and BisNP-$\frac{1}{2}$ adducts) or, in the case of C2N2 adduct, almost completely replaced by the novel band. These bands can be putatively attributed to the products formed by reduction of iminium intermediates **5** or enamine intermediates **6α/β** that are in equilibrium with ring-closed ribodiazepanes; however, the precise chemical structure of these products would require further investigations. Altogether, these results suggest an excellent stability of AP-X adducts in acidic and basic conditions, good tolerance with respect to strong nucleophiles (DTT, TCEP), and moderate stability in the presence of a strong reducing agent ($NaBH_4$).

The stability of the fU-X adduct prepared by the treatment of fU duplex with BisNP-NH was also assessed (Figure 10A). This adduct was partially degraded after treatment with 0.1 M HCl or 0.1 M NaOH (∼2-fold decrease after 25 min at 37°C),

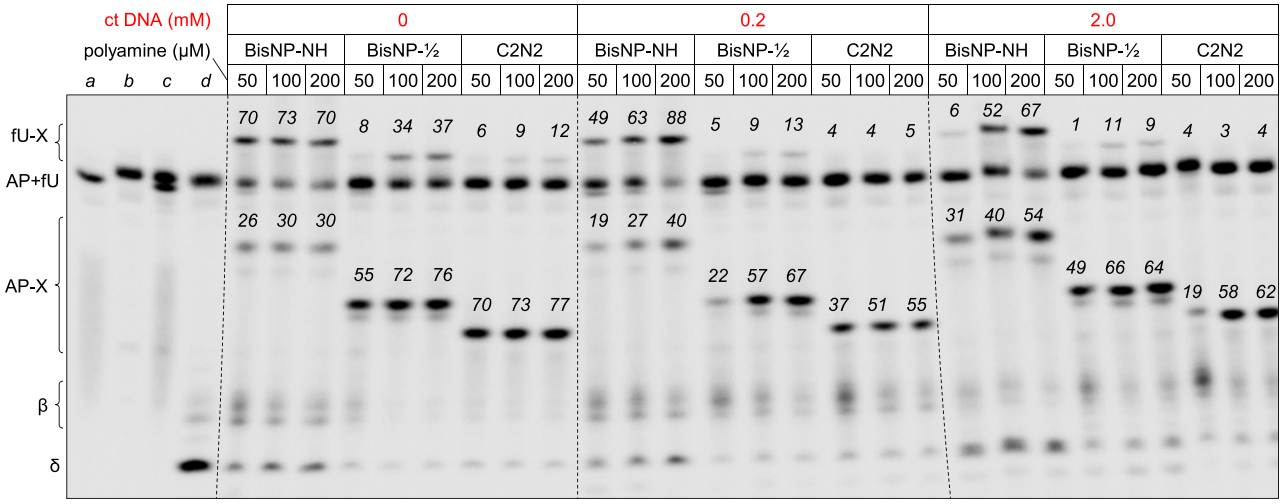

Figure 9. PAGE analysis of products obtained in reactions of an equimolar mixture of AP duplex and fU duplex (0.2 μM each) with BisNP-NH, BisNP-½, or C2N2 (50, 100 or 200 μM each) in the absence or in the presence of ct DNA (0.2 and 2 mM bp). Control lanes: (*a*) AP duplex only, (*b*) fU duplex only, (*c*) AP + fU duplex untreated, (*d*) AP + fU duplex treated with NaOH. The numbers in italics indicate the yields of AP-X and fU-X adducts with respect to the corresponding substrates (cf. Supplementary Note 2). Reaction time: 5 h, other conditions as in Figure 8.

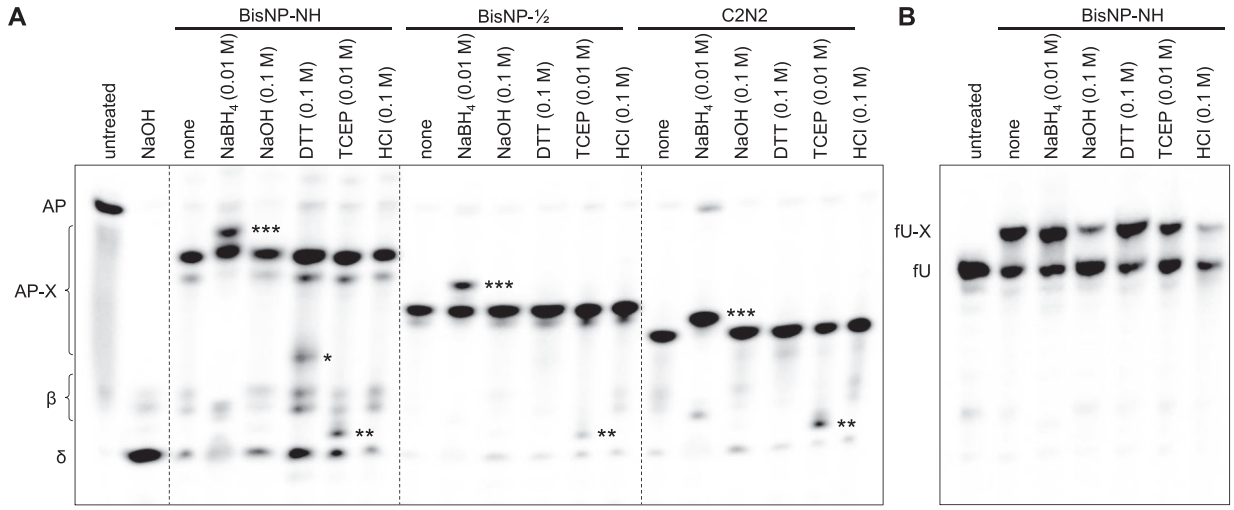

Figure 10. (**A**) Stability of AP-X adducts prepared by the treatment of AP duplex with BisNP-NH, BisNP-½, or C2N2 (10 μM each, 3 h at 37°C) upon incubation in the absence ('none') and in the presence of various reagents (25 min, 37°C). (**B**) Stability of the fU-X adduct prepared by the treatment of fU duplex with BisNP-NH (10 μM, 3 h at 37°C) upon incubation in the absence ('none') and in the presence of various reagents (25 min, 37°C). Initial conditions: 0.2 μM duplex substrate in 15 mM $KAsO_2Me_2$, 115 mM KCl buffer, pH 7.6.

but was essentially unaffected in the presence of $NaBH_4$, DTT and TCEP. Collectively, these results suggest that both AP-X and fU-X adducts are sufficiently stable to persist in physiological or near-physiological conditions and tolerate typical reagents used in biochemical workflows, and can therefore be used to develop chemical tools for labelling of AP sites and/or fU residues.

AP-X adducts represent roadblocks for APE1 and TDP1 enzymes

We were interested to study if 3′-ribodiazepane (AP-X) adducts could be removed by the enzymes of the base-excision DNA repair (BER) system. AP endonuclease 1 (APE1) cleaves the phosphodiester bond 5′ to AP sites leaving a 3′-OH residue and is equally able, albeit at a slower rate, to remove 3′-PUA, 3′-dR (β) remnants and bulky 3′-adducts due to its 3′→5′ exonuclease activity (83). However, the endonuclease activity of APE1 is completely blocked by oxime-type AP adducts that maintain the integrity of the phosphodiester backbone (37). Tyrosyl-DNA phosphodiesterase 1 (TDP1) hydrolyzes the phosphotyrosyl bond between the catalytic tyrosyl residue of topoisomerase 1 and DNA in topoisomerase-derived DPCs to leave a 3′-phosphate group (3′-P, δ), and is also able to cleanse a variety of 3′-blocking lesions including 3′-PUA and most synthetic DNA modifications (84,85). Recently, Yang *et al.* demonstrated that both APE1 and TDP1 were able to remove the oxime-type adduct of 3′-PUA with an aminooxy analogue of lysine (86,87); moreover, TDP1 was also able to remove a Michael-type DPC formed through the reaction of

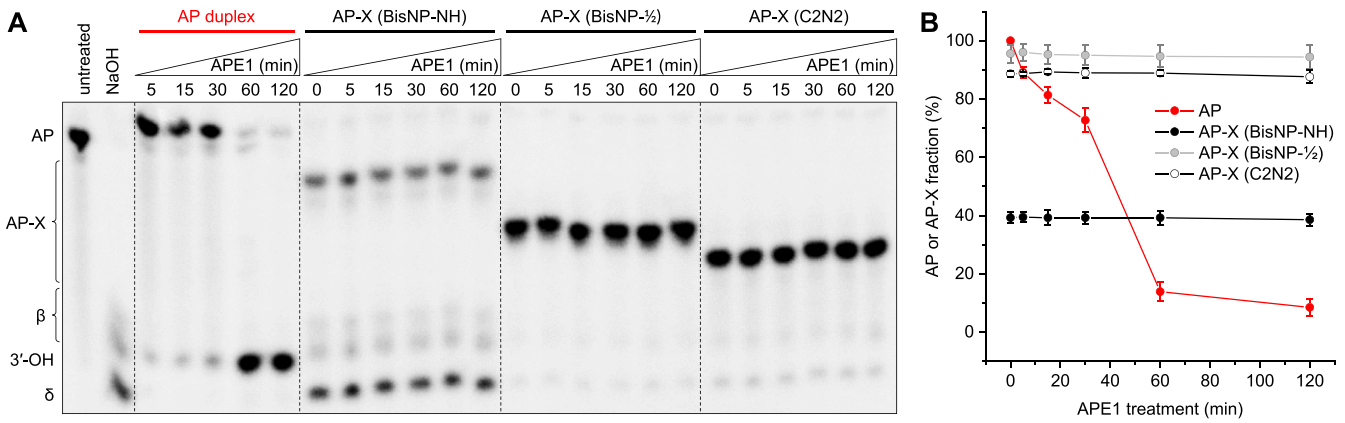

Figure 11. AP-X adducts are resistant towards APE1 treatment. (**A**) Representative PAGE analysis showing the effect of APE1 on the untreated AP duplex, or on AP duplexes pre-treated (3 h, 37°C) with BisNP-NH, BisNP-$\frac{1}{2}$, or C2N2 (10 μM each) to form the corresponding AP-X adducts. The AP strand was 5′-^{32}P-labelled. (**B**) Quantification of bands corresponding to the uncleaved AP substrate or AP-X adducts upon APE1 treatment, data are means ± s.d. from three independent experiments. Conditions: 0.2 μM substrate, 2.3 nM APE1 in 15 mM $KAsO_2Me_2$, 115 mM KCl, 1.7 mM $MgCl_2$ buffer, pH 6.5, $T = 37$°C.

3′-PUA with cysteine residue of ALKBH1 (88). Both these adducts are related to ribodiazepane AP-X adducts since they arise from the 3′-PUA intermediate upon cleavage of AP sites.

We studied the effect of APE1 on AP-X adducts formed by pre-treatment of AP duplex with BisNP-NH, BisNP-$\frac{1}{2}$, and C2N2 (Figure 11). Incubation with APE1 resulted in the cleavage of >80% of untreated AP duplex within 1 h, with concomitant formation of the 3′-OH product. However, if AP duplex was pre-treated with polyamines to generate AP-X adducts, the intensity of AP-X bands was not significantly reduced event after 2 h of APE1 treatment, indicating that AP-X adducts are resistant towards 3′-exonuclease activity of APE1.

Next, we investigated the effect of TDP1 on AP-X adducts. First, the activity of TDP1 was verified using duplex C12 (5-GTA/3-T(C_{12})C) containing a 1,12-dodecanediol spacer as a TDP1 substrate (89). Incubation of this duplex with TDP1 (0.5 μM) resulted in the cleavage of > 95% of the substrate within 30 min, with concomitant formation of the 3′-P product. When the reaction of the C12 duplex with TDP1 was performed in the presence of BisNP-NH, BisNP-$\frac{1}{2}$ or C2N2 (10 μM) the efficiency of the strand cleavage was slightly reduced; nevertheless, in all cases, >85% of substrate was cleaved after 1 h (Figure 12A, B). Assuming that these polyamines can non-covalently bind to C_{12} spacer sites (that represent close analogues of AP sites), this marginal inhibitory effect can be attributed to substrate-based (indirect) inhibition, i.e. competition of the polyamine with the enzyme for binding to the substrate (57). TDP1 was equally able to cleave AP sites in the untreated AP duplex (Supplementary Figure S23), in agreement with previous reports (90). Next, we studied the effect of TDP1 on AP-X adducts prepared by pre-treatment of the AP duplex with the three polyamines as described above. Remarkably, the intensity of the AP-X bands was not significantly reduced even after 1 h of TDP1 treatment (Figure 12C, D), indicating that TDP1 was unable to remove these adducts.

The finding that neither APE1 nor TDP1 are able to cleanse 3′ DNA termini bearing ribodiazepane adducts is rather surprising, because both enzymes are known to remove different types of adducts arising from 3′-PUA (34,86–88). We note that AP-X adducts employed as substrates were generated by using excess of polyamines (10 μM) that were not separated before enzymatic reactions and could, in principle, inhibit enzymatic activity. However, we have previously shown that BisNP-NH and its analogues do not directly interact with APE1 and inhibit the endonuclease activity exclusively through AP site binding (i.e. indirect) mechanism (57), and we also demonstrated here that all three polyamines only slightly inhibit TDP1 activity with respect to C12 substrate. Thus, the resistance of AP-X adducts towards APE1 and TDP1 cannot be attributed to interaction of polyamines with the enzymes. Instead, we can suggest that the bulky nature of ribodiazepane adducts, in particular the presence of two naphthyl groups, interferes with binding of the enzyme (or with the correct positioning of the substrate in the active site) and prevents the enzymatic reaction. Further investigations will address the binding of these enzymes to AP-X adducts and determine the actual mechanism of inhibition.

Conclusions

Both AP sites and fU are abundant DNA modifications that occur in the genome at comparable rates (46). Due to their aldehyde nature, they are prone to reactions with nucleophiles; however, until recently, the main reactivity of AP sites was considered to be due to the reversible formation of Schiff bases with lysine residues of proteins (21–23). Only recently other types of AP site reactivity were discovered, namely the formation of thiazolidines (19,20) and *S*-glycosylic derivatives (17,18) upon reaction with cysteine residues, as well as nucleophilic addition of exocyclic amino groups of neighboring nucleobases leading to the formation of *N*-glycosylic DNA ICLs (9–14). Likewise, most strategies developed for chemical labeling of AP sites rely on the formation of oxime adducts as stable analogues of Schiff bases, with the exception of recently developed chemical tools that employ iso-Pictet-Spengler reaction (50) or ABAO ligation (52). The reactivity of fU is even less studied, and only imine-type DPCs with nucleosomes have been documented so far (91–93). However, a number of chemical tools for labeling of fU have been developed, either through formation of oxime adducts or, more selectively, through formation of heterocycles or Knövenagel-type

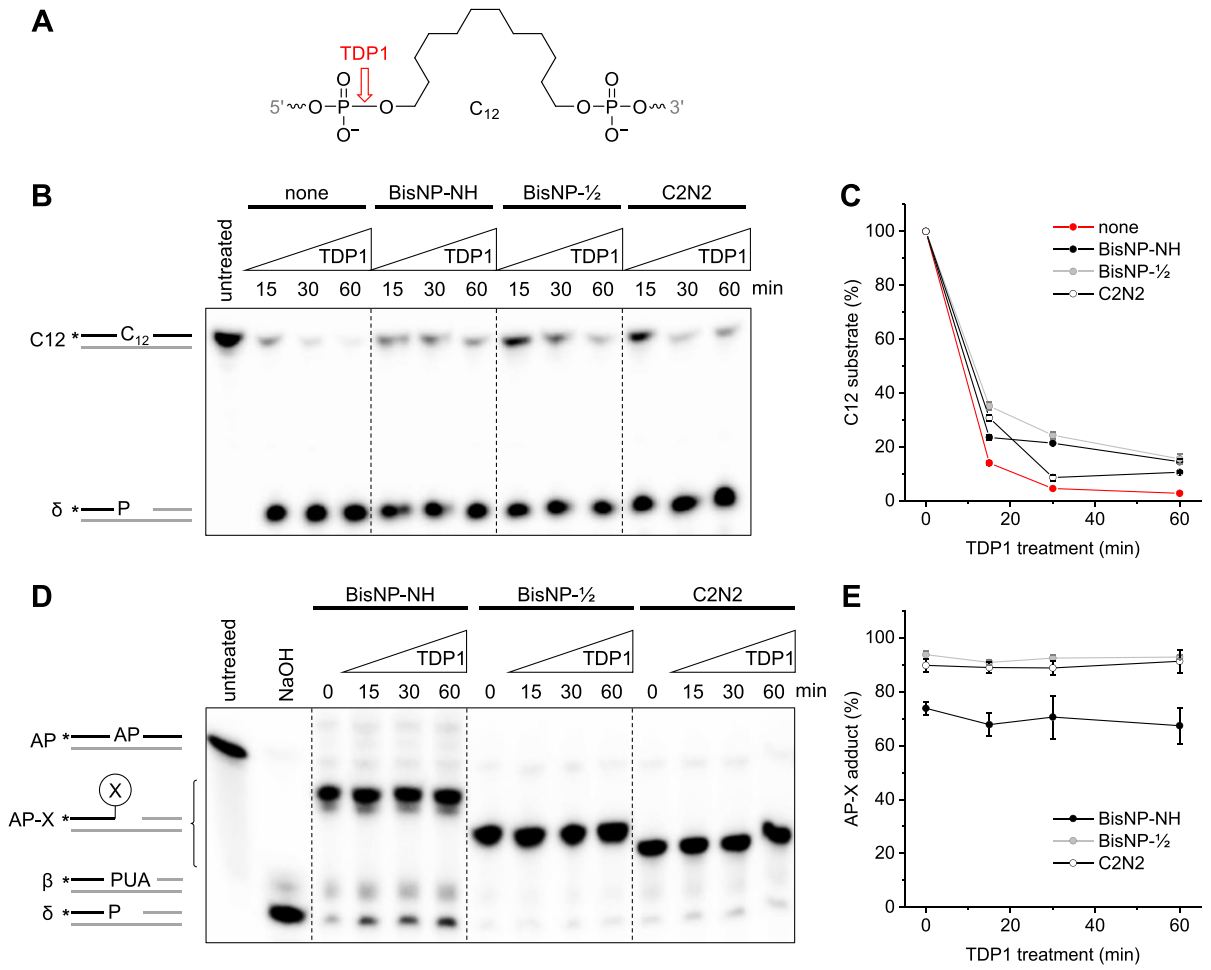

Figure 12. AP-X adducts are resistant towards TDP1 treatment. (**A**) Structure of DNA modification C_{12} employed as a model TDP1 substrate; the bond indicated with red arrow is hydrolytically cleaved by the enzyme. (**B**) Representative PAGE analysis showing the effect of TDP1 on the C12 duplex (the strand bearing a C_{12} modification was 5′-^{32}P-labelled) in the absence and in the presence of BisNP-NH, BisNP-$\frac{1}{2}$, and C2N2 (10 μM each). (**C**) Quantification of the bands of uncleaved C12 substrate upon TDP1 treatment (means ± s.d. from $N = 2$). (**D**) Representative PAGE analysis showing the effect of TDP1 on the AP duplex pre-treated (3 h, 37°C) with BisNP-NH, BisNP-$\frac{1}{2}$, or C2N2 (10 μM each) to form the corresponding AP-X adducts. (**E**) Quantification of the bands of AP-X adducts upon TDP1 treatment (means ± s.d. from $N = 2$). Conditions for the formation of AP-X substrate and TDP1 reactions: 0.2 μM substrate, 0.5 μM TDP1 in 50 mM Tris–HCl, 50 mM NaCl, 1 mM DTT buffer, pH 8.5, $T = 37$°C.

condensation reactions, enabling its fluorimetric detection and/or genomic mapping (53,56).

In this study, we describe an unprecedented reactivity of AP sites, fU and fC with polyamines, that results in the formation of stable covalent adducts in the absence of reducing agents. Using a set of polyamines derived from the macrocycle BisNP-NH, the first compound for which we serendipitously observed this type of reactivity (59), we demonstrate that the structural determinants for this reactivity include a secondary 1,2-diamine fragment along with the presence of benzene or, better, naphthalene residues whose role consists in enhancing the DNA binding by π-stacking interactions. Using small-molecule models, we elucidated the structures of the adducts formed in reactions with AP sites and fU residues. In the case of AP sites, 3′-ribodiazepane (AP-X) adducts are formed upon polyamine-induced AP site cleavage through an intramolecular cyclization of the iminium intermediate related to 3′-PUA; this implies that they can equally form upon reaction of polyamines with 3′-PUA residues provided the latter are sufficiently persistent. Conversely, the reaction of the same secondary 1,2-diamine fragment with fU residues leads to the formation of cationic 2,3-dihydro-1,4-diazepinium (fU-X) adducts through ring-opening of the uracil residue. We were not able to determine the structure of the fC-X product formed in reactions with fC residues due to low yields (≤5%) observed with all tested polyamines; further investigations are needed to determine whether fC-X represents a trivial 1,3-aminal, a product of cytosine ring-opening, or yet another structure.

An important finding of this work is the fact that AP-X adducts are rather chemically stable and, moreover, represents roadblocks for two DNA repair enzymes of the BER system, APE1 and TDP1, despite the fact that the latter is known to cleanse a wide variety of 3′-blocking DNA modifications including oxime-type and Michael-type adducts arising from 3′-PUA. To the best of our knowledge, ribodiazepane AP-X adducts is the first example of a 3′-blocking DNA modification unable to be resolved by TDP1. Since APE1 and TDP1 are two key enzymes involved in the repair of 3′-blocking DNA modifications (2), this suggests that cells deficient in alternative repair pathways capable of removing 3′-blocking lesions, such as nucleotide excision repair (94–96), can

potentially be sensitive to polyamines that effectively generate AP-X adducts, in particularly in combinations with DNA alkylating agents that produce transiently high levels of AP sites. In this regard it is interesting to note that one compound from our study, DBED, also known as Benzathine, is a pharmaceutical excipient widely used for the preparation of poorly soluble, long-acting salts of penicillin antibiotics (97,98), and DBDT has also been once proposed for this purpose (99). Although both compounds produce much lower yield of AP-X and fU-X adducts in comparison with the naphthalene analogues, our observations may call for a detailed assessment of potential genotoxic effects of DBED, in particular in combinations with DNA alkylating agents. Furthermore, the stability of AP-X adducts towards other DNA repair enzymes such as 3′ DNA repair endonuclease (TREX1), APE2, NEIL1/3 and ERCC1-XPF nuclease merits further investigations.

Finally, our study demonstrates that, although the structural determinants for reaction of polyamines with both AP site and fU residues are identical, the AP-vs.-fU selectivity can be finely tuned through variation of the chemical structure of the polyamine, on one hand, and reaction conditions such as pH of the medium, on the other hand. Thus, BisNP-NH shows a two-fold selectivity for fU versus AP sites in slightly acidic conditions (pH 6.5), whereas BisNP-$\frac{1}{2}$ and C2N2 preferentially react with AP sites, reaching a 20-fold AP-vs.-fU selectivity for C2N2 at pH 7.2. Moreover, the substrate selectivity of BisNP-$\frac{1}{2}$ and C2N2 remains unaffected when the reaction is performed in the presence of large excess of undamaged genomic DNA. Thus, this novel reaction can serve as a basis for development of methods allowing selective chemical labelling of AP sites in genome. Remarkably, the reaction of these polyamines with both AP sites and fU is fast ($\leq$1 h) in near-physiological conditions and at low-micromolar concentrations of polyamines, suggesting that it can also take place in living systems.

Data availability

The data underlying this article are available in the article and in its online supplementary material.

Supplementary data

Supplementary Data are available at NAR Online.

Acknowledgements

We thank Ms. Delphine Martin (CMBC) for help with NMR experiments and Ms. Leïla Chouh (CMBC) for help with the synthesis of BisNP-NH/O.

Funding

European Union's Horizon 2020 research and innovation programme under the Marie Skłodowska−Curie grant agreement [847718 (Institut Curie's EuReCa PhD Programme, PhD fellowship to E.P.G.N.P.)]; *Agence Nationale de la Recherche* through the Graduate School on Chemistry, Biology and Health (CBH-EUR-GS), University Grenoble Alpes [ANR-17-EURE-0003]. Y.P. is supported by the Center for Cancer Research, the Intramural Program of the National Cancer Institute [Z01-BC-006150]. Funding for open access charge: Institut Curie.

Conflict of interest statement

None declared.

References

1. Gates,K.S. (2009) An overview of chemical processes that damage cellular DNA: spontaneous hydrolysis, alkylation, and reactions with radicals. *Chem. Res. Toxicol.*, **22**, 1747–1760.
2. Hegde,M.L., Hazra,T.K. and Mitra,S. (2008) Early steps in the DNA base excision/single-strand interruption repair pathway in mammalian cells. *Cell Res.*, **18**, 27–47.
3. Krokan,H.E. and Bjoras,M. (2013) Base excision repair. *Cold Spring Harb. Perspect. Biol.*, **5**, a012583.
4. Thompson,P.S. and Cortez,D. (2020) New insights into abasic site repair and tolerance. *DNA Repair (Amst.)*, **90**, 102866.
5. Kim,Y.-J. and M. Wilson,D. III (2012) Overview of base excision repair biochemistry. *Curr. Mol. Pharmacol.*, **5**, 3–13.
6. Drohat,A.C. and Coey,C.T. (2016) Role of base excision "repair" enzymes in erasing epigenetic marks from DNA. *Chem. Rev.*, **116**, 12711–12729.
7. Wu,S.C. and Zhang,Y. (2010) Active DNA demethylation: many roads lead to Rome. *Nat. Rev. Mol. Cell Biol.*, **11**, 607–620.
8. Lhomme,J., Constant,J.F. and Demeunynck,M. (1999) Abasic DNA structure, reactivity, and recognition. *Biopolymers*, **52**, 65–83.
9. Dutta,S., Chowdhury,G. and Gates,K.S. (2007) Interstrand cross-links generated by abasic sites in duplex DNA. *J. Am. Chem. Soc.*, **129**, 1852–1853.
10. Johnson,K.M., Price,N.E., Wang,J., Fekry,M.I., Dutta,S., Seiner,D.R., Wang,Y. and Gates,K.S. (2013) On the formation and properties of interstrand DNA-DNA cross-links forged by reaction of an abasic site with the opposing guanine residue of 5′-CAp sequences in duplex DNA. *J. Am. Chem. Soc.*, **135**, 1015–1025.
11. Price,N.E., Johnson,K.M., Wang,J., Fekry,M.I., Wang,Y. and Gates,K.S. (2014) Interstrand DNA–DNA cross-link formation between adenine residues and abasic sites in duplex DNA. *J. Am. Chem. Soc.*, **136**, 3483–3490.
12. Price,N.E., Catalano,M.J., Liu,S., Wang,Y. and Gates,K.S. (2015) Chemical and structural characterization of interstrand cross-links formed between abasic sites and adenine residues in duplex DNA. *Nucleic Acids Res.*, **43**, 3434–3441.
13. Kellum,A.H., Qiu,D.Y., Voehler,M.W., Martin,W., Gates,K.S. and Stone,M.P. (2021) Structure of a stable interstrand DNA cross-link involving a β-*N*-glycosyl linkage between an N^6-dA amino group and an abasic site. *Biochemistry*, **60**, 41–52.
14. Amin,S.B.M., Islam,T., Price,N.E., Wallace,A., Guo,X., Gomina,A., Heidari,M., Johnson,K.M., Lewis,C.D., Yang,Z., *et al.* (2022) Effects of local sequence, reaction conditions, and various additives on the formation and stability of interstrand cross-links derived from the reaction of an abasic site with an adenine residue in duplex DNA. *ACS Omega*, **7**, 36888–36901.
15. Khodyreva,S. and Lavrik,O. (2020) Non-canonical interaction of DNA repair proteins with intact and cleaved AP sites. *DNA Repair (Amst.)*, **90**, 102847.
16. Nakamura,J. and Nakamura,M. (2020) DNA-protein crosslink formation by endogenous aldehydes and AP sites. *DNA Repair (Amst.)*, **88**, 102806.
17. Chan,W., Ham,Y.-H., Jin,L., Chan,H.W., Wong,Y.-L., Chan,C.-K. and Chung,P.-Y. (2019) Quantification of a novel DNA–protein cross-link product formed by reacting apurinic/apyrimidinic sites in DNA with cysteine residues in protein by liquid chromatography-tandem mass spectrometry coupled with the stable isotope-dilution method. *Anal. Chem.*, **91**, 4987–4994.
18. Ghodke,P.P., Matse,J.H., Dawson,S. and Guengerich,F.P. (2022) Nucleophilic thiol proteins bind covalently to abasic sites in DNA. *Chem. Res. Toxicol.*, **35**, 1805–1808.
19. Halabelian,L., Ravichandran,M., Li,Y., Zeng,H., Rao,A., Aravind,L. and Arrowsmith,C.H. (2019) Structural basis of

HMCES interactions with abasic DNA and multivalent substrate recognition. *Nat. Struct. Mol. Biol.*, **26**, 607–612.
20. Thompson,P.S., Amidon,K.M., Mohni,K.N., Cortez,D. and Eichman,B.F. (2019) Protection of abasic sites during DNA replication by a stable thiazolidine protein-DNA cross-link. *Nat. Struct. Mol. Biol.*, **26**, 613–618.
21. Zhao,W., Xu,W., Tang,J., Kaushik,S., Chang,C.-E.A. and Zhao,L. (2023) Key amino acid residues of mitochondrial transcription factor A synergize with abasic (AP) site dynamics to facilitate AP-lyase reactions. *ACS Chem. Biol.*, **18**, 1168–1179.
22. Sczepanski,J.T., Wong,R.S., McKnight,J.N., Bowman,G.D. and Greenberg,M.M. (2010) Rapid DNA–protein cross-linking and strand scission by an abasic site in a nucleosome core particle. *Proc. Natl. Acad. Sci. U.S.A.*, **107**, 22475–22480.
23. Zhou,C., Sczepanski,J.T. and Greenberg,M.M. (2012) Mechanistic studies on histone catalyzed cleavage of apyrimidinic/apurinic sites in nucleosome core particles. *J. Am. Chem. Soc.*, **134**, 16734–16741.
24. Yang,K., Park,D., Tretyakova,N.Y. and Greenberg,M.M. (2018) Histone tails decrease N7-methyl-2′-deoxyguanosine depurination and yield DNA–protein cross-links in nucleosome core particles and cells. *Proc. Natl. Acad. Sci. U.S.A.*, **115**, E11212–E11220.
25. Haldar,T., Jha,J.S., Yang,Z., Nel,C., Housh,K., Cassidy,O.J. and Gates,K.S. (2022) Unexpected complexity in the products arising from NaOH-, heat-, amine-, and glycosylase-induced strand cleavage at an abasic site in DNA. *Chem. Res. Toxicol.*, **35**, 218–232.
26. Yang,Z., Price,N.E., Johnson,K.M., Wang,Y. and Gates,K.S. (2017) Interstrand cross-links arising from strand breaks at true abasic sites in duplex DNA. *Nucleic Acids Res.*, **45**, 6275–6283.
27. Housh,K., Jha,J.S., Yang,Z., Haldar,T., Johnson,K.M., Yin,J., Wang,Y. and Gates,K.S. (2021) Formation and repair of an interstrand DNA cross-link arising from a common endogenous lesion. *J. Am. Chem. Soc.*, **143**, 15344–15357.
28. Nazarkina,Z.K., Khodyreva,S.N., Marsin,S., Lavrik,O.I. and Radicella,J.P. (2007) XRCC1 interactions with base excision repair DNA intermediates. *DNA Repair (Amst.)*, **6**, 254–264.
29. Kosova,A.A., Khodyreva,S.N. and Lavrik,O.I. (2015) Glyceraldehyde-3-phosphate dehydrogenase (GAPDH) interacts with apurinic/apyrimidinic sites in DNA. *Mutat. Res.*, **779**, 46–57.
30. Müller,T.A., Andrzejak,M.M. and Hausinger,R.P. (2013) A covalent protein–DNA 5′-product adduct is generated following AP lyase activity of human ALKBH1 (AlkB homologue 1). *Biochem. J.*, **452**, 509–518.
31. Müller,T.A., Tobar,M.A., Perian,M.N. and Hausinger,R.P. (2017) Biochemical characterization of AP lyase and m6A demethylase activities of Human AlkB homologue 1 (ALKBH1). *Biochemistry*, **56**, 1899–1910.
32. Xu,W., Tang,J. and Zhao,L. (2023) DNA–protein cross-links between abasic DNA damage and mitochondrial transcription factor A (TFAM). *Nucleic Acids Res.*, **51**, 41–53.
33. Wei,X. and Yang,K. (2023) PARP1 Incises abasic sites and covalently cross-links to 3′-DNA termini via cysteine addition not reductive amination. *Biochemistry*, **62**, 1527–1530.
34. Jha,J.S., Yin,J., Haldar,T., Yang,Z., Wang,Y. and Gates,K.S. (2022) Reconsidering the chemical nature of Strand breaks derived from abasic sites in cellular DNA: evidence for 3′-glutathionylation. *J. Am. Chem. Soc.*, **144**, 10471–10482.
35. Boturyn,D., Constant,J.-F., Defrancq,E., Lhomme,J., Barbin,A. and Wild,C.P. (1999) A simple and sensitive method for in vitro quantitation of abasic sites in DNA. *Chem. Res. Toxicol.*, **12**, 476–482.
36. Condie,A.G., Yan,Y., Gerson,S.L. and Wang,Y. (2015) A fluorescent probe to measure DNA damage and repair. *PLoS One*, **10**, e0131330.
37. Wei,S., Shalhout,S., Ahn,Y.H. and Bhagwat,A.S. (2015) A versatile new tool to quantify abasic sites in DNA and inhibit base excision repair. *DNA Repair (Amst.)*, **27**, 9–18.
38. Wilson,D.L. and Kool,E.T. (2019) Ultrafast oxime formation enables efficient fluorescence light-up measurement of DNA base excision. *J. Am. Chem. Soc.*, **141**, 19379–19388.
39. Tan,H., Li,X., Shi,M., Wang,J., Yang,Z. and Zhao,M. (2023) A homogeneous fluorescence assay for rapid and sensitive quantification of the global level of abasic sites in genomic DNA. *DNA Repair (Amst.)*, **122**, 103451.
40. Adamczyk,M., Mattingly,P.G., Moore,J.A. and Pan,Y. (1999) Synthesis of a chemiluminescent acridinium hydroxylamine (AHA) for the direct detection of abasic sites in DNA. *Org. Lett.*, **1**, 779–781.
41. Kubo,K., Ide,H., Wallace,S.S. and Kow,Y.W. (1992) A novel, sensitive, and specific assay for abasic sites, the most commonly produced DNA lesion. *Biochemistry*, **31**, 3703–3708.
42. Ide,H., Akamatsu,K., Kimura,Y., Michiue,K., Makino,K., Asaeda,A., Takamori,Y. and Kubo,K. (1993) Synthesis and damage specificity of a novel probe for the detection of abasic sites in DNA. *Biochemistry*, **32**, 8276–8283.
43. Nakamura,J., Walker,V.E., Upton,P.B., Chiang,S.Y., Kow,Y.W. and Swenberg,J.A. (1998) Highly sensitive apurinic/apyrimidinic site assay can detect spontaneous and chemically induced depurination under physiological conditions. *Cancer Res.*, **58**, 222–225.
44. Atamna,H., Cheung,I. and Ames,B.N. (2000) A method for detecting abasic sites in living cells: age-dependent changes in base excision repair. *Proc. Natl. Acad. Sci. U.S.A.*, **97**, 686–691.
45. Kojima,N., Takebayashi,T., Mikami,A., Ohtsuka,E. and Komatsu,Y. (2009) Construction of highly reactive probes for abasic site detection by introduction of an aromatic and a guanidine residue into an aminooxy group. *J. Am. Chem. Soc.*, **131**, 13208–13209.
46. Rahimoff,R., Kosmatchev,O., Kirchner,A., Pfaffeneder,T., Spada,F., Brantl,V., Müller,M. and Carell,T. (2017) 5-Formyl- and 5-carboxydeoxycytidines do not cause accumulation of harmful repair intermediates in stem cells. *J. Am. Chem. Soc.*, **139**, 10359–10364.
47. Chen,H., Yao,L., Brown,C., Rizzo,C.J. and Turesky,R.J. (2019) Quantitation of apurinic/apyrimidinic sites in isolated DNA and in mammalian tissue with a reduced level of artifacts. *Anal. Chem.*, **91**, 7403–7410.
48. Jun,Y.W., Albarran,E., Wilson,D.L., Ding,J. and Kool,E.T. (2022) Fluorescence imaging of mitochondrial DNA base excision repair reveals dynamics of oxidative stress responses. *Angew. Chem. Int. Ed.*, **61**, e202111829.
49. Poetsch,A.R., Boulton,S.J. and Luscombe,N.M. (2018) Genomic landscape of oxidative DNA damage and repair reveals regioselective protection from mutagenesis. *Genome Biol.*, **19**, 215.
50. Liu,Z.J., Martínez Cuesta,S., van Delft,P. and Balasubramanian,S. (2019) Sequencing abasic sites in DNA at single-nucleotide resolution. *Nat. Chem.*, **11**, 629–637.
51. Hardisty,R.E., Kawasaki,F., Sahakyan,A.B. and Balasubramanian,S. (2015) Selective chemical labeling of natural T modifications in DNA. *J. Am. Chem. Soc.*, **137**, 9270–9272.
52. Li,N., Zhou,Q., Li,K., Jiang,T. and Yu,X.-Q. (2023) Qualitative and quantitative detection of aldehydes in DNA with 2-amino benzamidoxime derivative. *Chin. Chem. Lett.*, **34**, 107471.
53. Wang,Y., Zhang,X., Zou,G., Peng,S., Liu,C. and Zhou,X. (2019) Detection and application of 5-formylcytosine and 5-formyluracil in DNA. *Acc. Chem. Res.*, **52**, 1016–1024.
54. Dai,Y., Yuan,B.-F. and Feng,Y.-Q. (2021) Quantification and mapping of DNA modifications. *RSC Chem. Biol.*, **2**, 1096–1114.
55. Liu,H., Wang,Y. and Zhou,X. (2022) Labeling and sequencing nucleic acid modifications using bio-orthogonal tools. *RSC Chem. Biol.*, **3**, 994–1007.
56. Yang,W., Han,S., Zhang,X., Wang,Y., Zou,G., Liu,C., Xu,M. and Zhou,X. (2021) Sequencing 5-formyluracil in genomic DNA at single-base resolution. *Anal. Chem.*, **93**, 15445–15451.
57. Kotera,N., Poyer,F., Granzhan,A. and Teulade-Fichou,M.-P. (2015) Efficient inhibition of human AP endonuclease 1 (APE1) via

substrate masking by abasic site-binding macrocyclic ligands. *Chem. Commun.*, **51**, 15948–15951.
58. Kotera,N., Granzhan,A. and Teulade-Fichou,M.-P. (2016) Comparative study of affinity and selectivity of ligands targeting abasic and mismatch sites in DNA using a fluorescence-melting assay. *Biochimie*, **128–129**, 133–137.
59. Caron,C., Duong,X.N.T., Guillot,R., Bombard,S. and Granzhan,A. (2019) Interaction of functionalized naphthalenophanes with abasic sites in DNA: DNA cleavage, DNA cleavage inhibition, and formation of ligand–DNA adducts. *Chem. Eur. J.*, **25**, 1949–1962.
60. Granzhan,A., Largy,E., Saettel,N. and Teulade-Fichou,M.-P. (2010) Macrocyclic DNA-mismatch-binding ligands: structural determinants of selectivity. *Chem. Eur. J.*, **16**, 878–889.
61. Petitjean,A., Cuccia,L.A., Schmutz,M. and Lehn,J.-M. (2008) Naphthyridine-based helical foldamers and macrocycles: synthesis, cation binding, and supramolecular assemblies. *J. Org. Chem.*, **73**, 2481–2495.
62. Galaup,C., Couchet,J.-M., Bedel,S., Tisnès,P. and Picard,C. (2005) Direct access to terpyridine-containing polyazamacrocycles as photosensitizing ligands for Eu(III) luminescence in aqueous Media. *J. Org. Chem.*, **70**, 2274–2284.
63. Jha,J.S., Nel,C., Haldar,T., Peters,D., Housh,K. and Gates,K.S. (2022) Products generated by amine-catalyzed strand cleavage at apurinic/apyrimidinic sites in DNA: new insights from a biomimetic nucleoside model system. *Chem. Res. Toxicol.*, **35**, 203–217.
64. Zott,F.L., Korotenko,V. and Zipse,H. (2022) The pH-dependence of the hydration of 5-formylcytosine: an experimental and theoretical study. *ChemBioChem*, **23**, e202100651.
65. Antony,S., Marchand,C., Stephen,A.G., Thibaut,L., Agama,K.K., Fisher,R.J. and Pommier,Y. (2007) Novel high-throughput electrochemiluminescent assay for identification of human tyrosyl-DNA phosphodiesterase (Tdp1) inhibitors and characterization of furamidine (NSC 305831) as an inhibitor of Tdp1. *Nucleic Acids Res.*, **35**, 4474–4484.
66. Catalano,M.J., Price,N.E. and Gates,K.S. (2016) Effective molarity in a nucleic acid-controlled reaction. *Bioorg. Med. Chem. Lett.*, **26**, 2627–2630.
67. Jurčık,V. and Wilhelm,R. (2004) Preparation of aminals in water. *Tetrahedron*, **60**, 3205–3210.
68. Buchs,B., Godin,G., Trachsel,A., De Saint Laumer,J.Y., Lehn,J.M. and Herrmann,A. (2011) Reversible aminal formation: controlling the evaporation of bioactive volatiles by dynamic combinatorial/covalent chemistry. *Eur. J. Org. Chem.*, **2011**, 681–695.
69. Jash,A., Paliyath,G. and Lim,L.-T. (2018) Activated release of bioactive aldehydes from their precursors embedded in electrospun poly(lactic acid) nonwovens. *RSC Adv.*, **8**, 19930–19938.
70. Hwang,J.-T., Tallman,K.A. and Greenberg,M.M. (1999) The reactivity of the 2-deoxyribonolactone lesion in single-stranded DNA and its implication in reaction mechanisms of DNA damage and repair. *Nucleic Acids Res.*, **27**, 3805–3810.
71. Serrano,J.A., Jiménez,M. and Román,E. (1997) Preparation of new nucleoside analogues from 3,6-anhydrosugars. *J. Carbohydr. Chem.*, **16**, 1051–1059.
72. Lloyd,D., Cleghorn,H.P. and Marshall,D.R. (1974) 2,3-Dihy dro-1,4-diazepines. *Adv. Heterocycl. Chem.*, **17**, 1–26.
73. Lloyd,D., Tucker,K.S. and Marshall,D.R. (1981) Diazepines. Part 25. Preparation and properties of 6-aryl-2,3-dihydro-1,4-diazepinium salts. Electronic interaction between the rings and steric inhibition thereof. *J. Chem. Soc. Perkin Trans. 1*, **1981**, 726–735.
74. Barnett,C., Cleghorn,H.P., Cross,G.E., Lloyd,D. and Marshall,D.R. (1966) Diazepines. Part IV. Dihydrodiazepinium salts from the condensation reaction between *NN′*-disubstituted ethylenediamines and β-dicarbonyl compounds. *J. Chem. Soc. C*, **1966**, 93–95.
75. Lloyd,D. and McNab,H. (1976) Vinamidines and vinamidinium salts — Examples of stabilized push-pull alkenes. *Angew. Chem. Int. Ed.*, **15**, 459–468.
76. Hirota,K., Kitade,Y., Shimada,K. and Maki,Y. (1985) Pyrimidines. 54. Ring transformation of 5-(2-carbamoylvinyl)uracil derivatives to 5-carbamoylpyridin-2-ones. *J. Org. Chem.*, **50**, 1512–1516.
77. Singh Dolly,H., Singh Chimni,S. and Kumar,S. (1995) Acid catalysed enamine induced transformations of 1,3-dimethyl-5-formyluracil. A unique annulation reaction with enaminones. *Tetrahedron*, **51**, 12775–12780.
78. Singh,H., Singh,P., Chimni,S.S. and Kumar,S. (1995) Heterocyclic transformations. Part 7. Unprecedented transformations of 1,3-dialkyl-5-formyluracils to 1,3-dialkyl-7-hydroxyquinazolines. *J. Chem. Soc. Perkin Trans. 1*, **1995**, 2363–2367
79. Singh,H., Dolly,C. S.S. and Kumar,S. (1998) Enamine-induced ring transformations of 6-substituted 5-formyl-1,3-dimethyluracils. *J. Chem. Res.*, **1998**, 352–353.
80. Mityuk,A., Volochnyuk,D., Ryabukhin,S., Plaskon,A., Shivanyuk,A. and Tolmachev,A. (2009) Recyclization reactions of 5-formyl-1,3-dimethyluracil with electron-rich amino heterocycles. *Synthesis*, **2009**, 1858–1864.
81. Sochacka,E. and Smuga,D. (2007) Uracil ring opening in the reaction of 5-formyl-2′-deoxyuridine with primary alkyl amines. *Tetrahedron Lett.*, **48**, 1363–1367.
82. Kantner,T. and Watts,A.G. (2016) Characterization of reactions between water-soluble trialkylphosphines and thiol alkylating reagents: implications for protein-conjugation reactions. *Bioconjug. Chem.*, **27**, 2400–2406.
83. Whitaker,A.M. and Freudenthal,B.D. (2018) APE1: a skilled nucleic acid surgeon. *DNA Repair (Amst.)*, **71**, 93–100.
84. Pommier,Y., Huang,S.N., Gao,R., Das,B.B., Murai,J. and Marchand,C. (2014) Tyrosyl-DNA-phosphodiesterases (TDP1 and TDP2). *DNA Repair (Amst.)*, **19**, 114–129.
85. Sun,Y., Saha,S., Wang,W., Saha,L.K., Huang,S.Y.N. and Pommier,Y. (2020) Excision repair of topoisomerase DNA-protein crosslinks (TOP-DPC). *DNA Repair (Amst.)*, **89**, 102837.
86. Wei,X., Wang,Z., Hinson,C. and Yang,K. (2022) Human TDP1, APE1 and TREX1 repair 3′-DNA-peptide/protein cross-links arising from abasic sites in vitro. *Nucleic Acids Res.*, **50**, 3638–3657.
87. Bryan,C., Le,J., Wei,X. and Yang,K. (2023) *Saccharomyces cerevisiae* apurinic/apyrimidinic endonuclease 1 repairs abasic site-mediated DNA-peptide/protein cross-links. *DNA Repair (Amst.)*, **126**, 103501.
88. Wei,X., Person,M.D. and Yang,K. (2022) Tyrosyl-DNA phosphodiesterase 1 excises the 3′-DNA-ALKBH1 cross-link and its application for 3′-DNA-ALKBH1 cross-link characterization by LC-MS/MS. *DNA Repair (Amst.)*, **119**, 103391.
89. Lebedeva,N.A., Anarbaev,R.O., Kupryushkin,M.S., Rechkunova,N.I., Pyshnyi,D.V., Stetsenko,D.A. and Lavrik,O.I. (2015) Design of a new fluorescent oligonucleotide-based assay for a highly specific real-time detection of apurinic/apyrimidinic site cleavage by tyrosyl-DNA phosphodiesterase 1. *Bioconjug. Chem.*, **26**, 2046–2053.
90. Lebedeva,N.A., Rechkunova,N.I. and Lavrik,O.I. (2011) AP-site cleavage activity of tyrosyl-DNA phosphodiesterase 1. *FEBS Lett.*, **585**, 683–686.
91. Zou,G., Liu,C., Zeng,W., Yang,W., Zhang,K., Xie,Y., Chen,C. and Zhou,X. (2020) Regulable DNA–Protein interactions in vitro and vivo at epigenetic DNA marks. *CCS Chem.*, **2**, 54–63.
92. Zou,G., Zhang,K., Yang,W., Liu,C., Fang,Z. and Zhou,X. (2021) 5-Formyluracil targeted biochemical reactions with proteins inhibit DNA replication, induce mutations and interference gene expression in living cells. *Chin. Chem. Lett.*, **32**, 3252–3256.
93. Runtsch,L.S., Stadlmeier,M., Schön,A., Müller,M. and Carell,T. (2021) Comparative nucleosomal reactivity of 5-formyl-uridine and 5-formyl-cytidine. *Chem. Eur. J.*, **27**, 12747–12752.

94. Fisher,L.A., Samson,L. and Bessho,T. (2011) Removal of reactive oxygen species-induced 3′-blocked ends by XPF-ERCC1. *Chem. Res. Toxicol.*, **24**, 1876–1881.
95. Kitsera,N., Rodriguez-Alvarez,M., Emmert,S., Carell,T. and Khobta,A. (2019) Nucleotide excision repair of abasic DNA lesions. *Nucleic Acids Res.*, **47**, 8537–8547.
96. Kumar,N., Raja,S. and Van Houten,B. (2020) The involvement of nucleotide excision repair proteins in the removal of oxidative DNA damage. *Nucleic Acids Res.*, **48**, 11227–11243.
97. Fletcher,A.P. and Knappett,C.R. (1953) N,N′-dibenzylethylene-diamine penicillin: a new repository form of penicillin. *BMJ*, **1**, 188–189.
98. Kaplan,E.L. (2012) Benzathine penicillin G: a documentably important antibiotic in need of a tune-up?*Pediatr. Infect. Dis. J.*, **31**, 726–728.
99. Boissier,J.R., Combes,G. and Ratouis,R. (1967) FR1473885A: nouvelle triamine et ses sels,et procédé de préparation.

Received: May 23, 2023. **Revised:** September 14, 2023. **Editorial Decision:** September 15, 2023. **Accepted:** September 20, 2023